Master in Chemical Engineering

Development of NAM-FISH for the study of biofilms formed in an advanced 3D substrate

Master dissertation

of

Sofia Rocha da Cruz

Supervisor at FEUP: **Andreia S. Azevedo**

Joint supervisor at FEUP: **Nuno F. Azevedo**

Coordinator at Bac^{3}Gel: **Daniela P. Pacheco**

August 2023


ALiCE
ASSOCIATE
LABORATORY
IN CHEMICAL
ENGINEERING


lepabe
Laboratory for Process Engineering,
Environment, Biotechnology and Energy


B
E
L
Biofilm
Engineering
Lab

Acknowledgments

Six years flew by since I first set foot at FEUP and, at last, I could not be more grateful for having had the opportunity of growing here, by learning with and from some remarkable people. I believe it is time to say a few thank yous...

To my supervisor, Andreia, for the unconditional support throughout this semester, from whom I have learned a lot about what it is to be a great person and professional.

Thank you to my co-supervisors, Prof. Nuno Azevedo, for the assertive words and the instigation of creativity, and Daniela Pacheco, for all the knowledge shared and the kind words.

I would also like to thank all that shared the laboratories with me during the course of this work, for always being ready to assist.

To all my friends, for what we have lived in this house, for the mutual support. I am greatful for all the memories and eager to make new ones.

Thanks to my cousin Carlos, for the availability and good counseling, for continuously showing me what it is to be an engineer.

A thank you to my family, to my parents, for everything.

Sofia Cruz

Funding

This work was financially supported by: LA/P/0045/2020 (ALiCE), UIDB/00511/2020 and UIDP/00511/2020 (LEPABE), funded by national funds through FCT/MCTES (PIDDAC); e.Biofilm project (Grant agreement ID: 101087568), financed by HORIZON Coordination and Support Actions (HORIZON-WIDERA-2022-TALENTS-01).

Abstract

Biofilms have great impact in the medical field as they hinder the treatment of bacterial infections due to their distinctive lifestyle characteristics [1]. Cystic fibrosis (CF) is commonly associated with persistent polymicrobial biofilm infections that eventually lead to premature death [2]. Hence, it is very important to develop new models/platforms and methods to study biofilms, in order to better understand them and develop targeted strategies for preventing and treating biofilm-related infections.

In this work, the main goal was to implement and validate the Locked Nucleic Acid/2'-O- Methyl-Fluorescence *in situ* Hybridization (LNA/2'OMe-FISH) method on biofilms cultured in a novel substrate - Universal-Bac^{3}Gel -, which reproduces key properties of the human mucus. Two relevant pathogens in CF were selected, namely *Pseudomonas aeruginosa* (*P. aeruginosa*) and *Klebsiella pneumoniae* (*K. pneumoniae*), to generate single- and dual-species biofilms. Additionally, this technique was combined with confocal laser scanning microscopy (CLSM) to determine spatial distribution of *P. aeruginosa* and *K. pneumoniae* within the biofilm and to infer about their interactions.

The validation of the method was successfully accomplished since it revealed that LNA/2'OMe- FISH was capable of detecting around 84% of the cells detected by DAPI, with a correlation coefficient of 0.969 between the two methods. The implementation of LNA/2'OMe-FISH in single- species biofilms revealed that both species were able to form biofilms and reach a total number of cells detected by this method around log 8.9 and log 8.6 cells/mL, for *P. aeruginosa* and *K. pneumoniae*, respectively. Regarding growth time, *P. aeruginosa* presented higher counts at 48h of culture, while *K. pneumoniae* at 24h. Concerning dual-species biofilms, it was observed that these species were able to form biofilm and reach values of total cells (detected by LNA/2'OMe-FISH) similar to those achieved in single-species, around log 8.6 and log 8.2 cells/mL, for *P. aeruginosa* and *K. pneumoniae*, respectively. Therefore, both species revealed ability to form biofilms in the Universal-Bac^{3}Gel substrate. Through the combination of LNA/2'OMe-FISH with CLSM, it was possible to conclude that the species were mixed in the volume of the analyzed biofilm sample and therefore exhibit a co-aggregation distribution. This organization suggests that the two species present synergistic interactions, meaning that this consortium might benefit each species or, at the very least, be neutral to them.

Overall, it was clear that Universal-Bac^{3}Gel is able to sustain the growth of two common pathogens of CF, and that LNA/2'OMe-FISH allied with CLSM is a reliable and robust technique for cell discrimination, quantification and spatial localization of species within biofilms. Future work will focus on the employment of higher customized advanced substrates for enhanced recreation of CF airway environment for polymicrobial biofilm formation, performance of pre-colonization assays closely recreating CF infections timelines, antimicrobial susceptibility assays with clinically relevant antibiotics and implementation of LNA/2'OMe-FISH in real CF airway mucus samples for spatial organization assessment through CLSM.

Keywords: Biofilms, LNA/2'OMe-FISH, *P. aeruginosa*, *K. pneumoniae*, Universal-Bac^{3}Gel, CLSM

Resumo

Os biofilmes têm grande impacte na medicina porque eles dificultam o tratamento de infeções bacterianas, devido às suas distintas características [1]. A fibrose quística (FQ) é uma doença frequentemente associada a infeções polimicrobianas persistentes, que acabam por conduzir à morte prematura [2]. Desta forma, é muito importante desenvolver novos modelos/plataformas e métodos para estudar biofilmes, a fim de os compreender melhor e desenvolver novas estratégias para prevenção e tratamento de infeções causadas por biofilmes.

No presente trabalho, o principal objetivo foi implementar e validar o método Locked Nucleic Acid/2'-O-Methyl-Fluorescence *in situ* Hybridization (LNA/2'OMe-FISH) em biofilmes desenvolvidos num novo substrato – Universal-Bac^{3}Gel – que reproduz propriedades essenciais do muco humano. Para tal, foram selecionados dois microrganismos patogénicos relevantes na FQ, nomeadamente *Pseudomonas aeruginosa* (*P. aeruginosa*) e *Klebsiella pneumoniae* (*K. pneumoniae*), para formar biofilmes simples e duplos. Além disso, esta técnica foi combinada com microscopia confocal de varredura a laser (CLSM) para determinar a distribuição espacial de *P. aeruginosa* e *K. pneumoniae* no biofilme duplo de modo a concluir sobre as suas interações.

A validação do método foi realizada com sucesso, uma vez que revelou que o LNA/2'OMe-FISH foi capaz de detetar cerca de 84% das células detetadas pelo DAPI, com um coeficiente de correlação de 0,969 entre os dois métodos. A implementação do LNA/2'OMe-FISH nos biofilmes revelou que ambas as espécies foram capazes de formar biofilmes simples e atingir um número total de células detetadas por este método cerca de log 8,9 e log 8,6 células/mL, para *P. aeruginosa* e *K. pneumoniae*, respetivamente. Relativamente ao tempo de crescimento de biofilme, a *P. aeruginosa* apresentou contagens mais elevadas às 48h de cultura, enquanto a *K. pneumoniae* apresentou contagens mais elevadas às 24h. Relativamente aos biofilmes duplos, observou-se que estas espécies foram capazes de formar biofilme e atingir valores de células totais (detetadas por LNA/2'OMe-FISH) semelhantes aos alcançados em biofilmes simples, cerca de log 8,6 e log 8,2 células/mL, para *P. aeruginosa* e *K. pneumoniae*, respetivamente. Deste modo, ambas as espécies revelaram capacidade para formar biofilmes no substrato Universal-Bac^{3}Gel. Através da combinação do LNA/2'OMe-FISH com CLSM, foi possível concluir que as espécies se encontravam misturadas no volume de biofilme analisado, apresentando assim uma distribuição em co-agregação. Esta organização sugere que as duas espécies apresentam interações sinérgicas, o que significa que este consórcio pode beneficiar cada uma das espécies ou, pelo menos, ser neutro.

No geral, comprovou-se que o substrato Universal-Bac^{3}Gel é capaz de sustentar o crescimento destes dois agentes patogénicos da FQ, e que o LNA/2'OMe-FISH aliado à CLSM se revelou uma técnica fiável e robusta para a discriminação celular, quantificação e localização espacial de espécies em biofilmes. Futuros trabalhos poderão centrar-se na utilização de outros substratos avançados que recriem com ainda maior fiabilidade as características encontradas nas vias respiratórias de pacientes de FQ para formação de biofilmes polimicrobianos, na realização de ensaios de pré-colonização recriando a ordem cronológica natural das infeções, na realização de ensaios de suscetibilidade antimicrobiana com antibióticos clinicamente relevantes e na implementação do LNA/2'OMe-FISH em amostras reais de muco das vias respiratórias da FQ para avaliação da organização espacial através de CLSM.

Palavras-chave: Biofilmes, LNA/2'OMe-FISH, *P. aeruginosa*, *K. pneumoniae*, Universal-Bac^{3}Gel, CLSM

Declaration

I hereby declare, under word of honor, that this work is original and that all non-original contributions are indicated, and due reference is given to the author and source.

Sofia Cruz

July 2023

Contents

List of Figures

List of Tables

Notation and Glossary

A_{image}	Area of the acquired images by microscopy (cm^2)
A_{well}	Area of the well of the microscopic slide (cm^2)
CFU_{counts}	Average of CFU counts
$Counts$	Averaged LNA/2'OMe-FISH or DAPI counts
d	Dilution of counted CFU
$D_{x,t}$	Dilution factor inherent to each biofilm; t corresponds to the biofilm development time and x corresponds to the type of biofilm (single- or dual-species)
F	Dilution factor
G'	Storage/elastic modulli (Pa)
G''	Loss/viscous modulli (Pa)
G^*	Complex modulus (Pa)
V	Volume of the sample used to plate the bacteria (μL)
V_{well}	Volume of the well of the microscopic slide (mL)

Greek Letters

δ	Phase angle between stress application and stress response; ranges from 0º to 90º

List of Acronyms

2'OMe	2'-O-Methyl
BRT	Biofilm Ring Device
CARD-FISH	Catalyzed Reporter Deposition-Fluorescence *in situ* Hybridization
CBD	Calgary Biofilm Device
CF	Cystic Fibrosis
CFU	Colony Forming Units
CLASI-FISH	Combinatorial Labelling and Spectral Imaging–Fluorescence *in situ* Hybridization
CLSM	Confocal Laser Scanning Microscopy
CV	Crystal Violet
CW	Chronic Wound
DFBR	Drip Flow Biofilm Reactor
DNA	Deoxyribonucleic Acid
eDNA	Extracellular DNA
EPS	Extracellular Polymeric Substances

FCM	Flow Cytometry
GFP	Green Fluorescent Protein
HGT	Horizontal Gene Transfer
LNA	Locked Nucleic Acid
MAR-FISH	MicroAutoRadiography-Fluorescence *in situ* Hybridization
MDR	Multidrug Resistance
NAM-FISH	Nucleic Acid Mimic-Fluorescence *in situ* Hybridization
NGS	Next Generation Sequencing
PI	Propidium Iodide
PNA	Peptide Nucleic Acid
RNA	Ribonucleic Acid
rRNA	Ribosomal RNA
RNAseq	RNA Sequencing
RT-qPCR	Reverse Transcriptase-quantitative Polymerase Chain Reaction
v-qPCR	Viable-quantitative Polymerase Chain Reaction
VBNC	Viable But Non-Culturable

1 Introduction

1.1 Framing and Presentation of the Work

The relevance of biofilms in the world, either for beneficial or detrimental reasons, is incontestable [8]. Research on biofilm mechanisms and dynamics is imperative in order to understand how we can use them in our favor or prevent/control them. Particularly, biofilms remain one of the greatest threats to human health, being responsible for the aggravation of health conditions and the cause of chronic infections [9].

The study of biofilms primarily involves two main stages: biofilm culture, which refers to the initial colonization and growth of bacteria on a surface, and subsequent biofilm analysis, which involves examining and studying the developed biofilm. Research in the field of biofilms has rapidly increased since its most accepted description in 2002 [10], but limitations of the existing analytical methods were soon exposed. Most limitations are related to the difficulty in mimicking natural *in vivo* conditions. In this study, a novel advanced 3D substrate - Universal-Bac^{3}Gel - was used to culture single- and dual-species biofilms. This substrate has a mucus bioinspired chemistry and provides an oxygen and nutrient gradient, ideal for culturing biofilms with metabolically diverse microorganisms [11].

Regarding the analysis of biofilms, many techniques are available and can be selected depending on the aim of the study (e.g., evaluating biofilms matrix components, assess cell viability, cell quantification, biofilm formation dynamics, cell interactions). The combination of different analytical techniques is usually done to achieve higher robustness [12, 13].

Fluorescence *in situ* hybridization (FISH) is one of the most powerful, widely employed approaches for targeting microorganisms [14]. FISH advantages are undeniable, but one of the most significant is that hybridization is performed *in situ* and therefore does not require sample destruction. The traditional FISH technique is constantly undergoing improvements, with new, more versatile and robust FISH variants emerging regularly [15]. In this work, LNA/2'OMe-FISH was implemented, where nucleic acid mimics (NAM) are used as probes [16]. In the case of biofilms, LNA/2'OMe-FISH might be combined with CLSM for *in situ* visualization and localization of different species within the biofilm [3].

As such, the main goal of this work involved the implementation and validation of LNA/2'OMe-FISH method to assess the spatial organization of biofilms grown in an advanced 3D substrate (Universal-Bac^{3}Gel). As a case study, two microorganisms from the ESKAPE pathogens group that are also relevant in CF airways infections, were selected to form single- and dual-species biofilms, namely *P. aeruginosa* and *K. pneumoniae*.

1.2 Company Presentation

The present work was conducted in a two entities partnership by taking advantage of two novel methods in which the involved institutions are pioneers. The work was developed in FEUP, at LEPABE (BEL group) laboratories, in partnership with Bac^{3}Gel - a Biotech startup whose mission is the generation of novel substrates that closely mimic natural environments for culturing microorganisms.

1.3 Main Contributions

The present work was fully performed and written by me. Bac^{3}Gel has provided the advanced culturing substrates used in this research. Rheological characterization of the substrates presented was performed by Daniela P. Pacheco, co-founder and CTO at Bac^{3}Gel, alongside with the substrates properties.

1.4 Document Structure

The present chapter includes the presentation of the work, a brief presentation of the entities involved, the main contributions and the document structure.

Chapter 2 comprises the context and state of the art. Section 2.1 addresses the basic concepts of biofilms, including its history, definition, formation mechanisms and properties, followed by Section 2.2 that narrates the role of biofilms in health. Section 2.3 provides an overview of the available and most widely used platforms (Subsection 2.3.1) and methods (Subsection 2.3.2) for studying biofilms. Section 2.4 unveils the most relevant technique for the present work, Fluorescence *in situ* Hybridization (FISH), specifically, its variant Nucleic Acid Mimics-FISH (NAM-FISH).

Chapter 3 contains a detailed description of the material and methods implemented during the course of the experiments.

Chapter 4 addresses the results obtained accompanied by its discussion. The topics delved into are the validation of the method, the quantification of biofilm growth, and the spatial organization of the formed biofilms.

Chapter 5 presents the main conclusions obtained from the present work and highlights some perspectives for the future of this research topic.

2 Context and State of the art

2.1 Basic Concepts of Biofilms: History, Definition and Formation

Biofilms are the most common and preferred mode of bacterial growth in nature and can be found in the most distinct places, whether it is in our mouth or deep-sea vents. Also, biofilms are not a recent lifeform since there is evidence of microbial biofilms existing in the Precambrian era [17]. The fact that biofilms have persisted through all these time periods on earth reveals their resilience, versatility and adaptation capacity [18].

For a long time, our knowledge of biofilms was very limited. In fact, for many years, bacteria were perceived as free-floating single cells or as we might call it now, living in the planktonic state [19]. This general idea started to crumble down when curiosity stroke and an exciting new observation was made. More precisely, in 1674, the Dutch scientist and inventor of the microscope, Anton Van Leeuwenhoek reported the observation of microbial aggregates from a sample of dental plaque scraped from his mouth [20, 8]. Many years went by and few observations of these aggregates were made. In the meantime, Louis Pasteur reported and sketched aggregates of bacteria that were the cause of wine spoilage [21]. In 2002, Donlan and Costerton presented one of the most widely accepted descriptions of the term “biofilm” to date, which was “a microbially derived sessile community characterized by cells that are irreversibly attached to a substrate or interface or to each other, are embedded in a matrix of extracellular polymeric substances that they have produced and exhibit an altered phenotype with respect to growth rate and gene transcription“ [10].

Since the definition of biofilms became well-established, an exponential amount of research has been conducted on the topic. Thereafter, many efforts have been made to understand why cells prefer the sessile lifestyle over the planktonic, what properties emerge from this arrangement and how do cells organize themselves within this communities [8].

Nowadays, biofilms can be defined as well-structured, cooperating communities of microorganisms adhered to a surface, either biotic or abiotic, embedded in a self-produced matrix. The majority of naturally occurring biofilms are multispecies and highly diverse, presenting high cell density and different organizations [22, 8, 23]. A high number of microbes have been documented to form biofilms, namely prokaryotes such as bacteria, archaea [24], and eukaryotes including fungi [25] and microalgae [26].

The great success associated with this sessile life form derives greatly from its extracellular matrix. In fact, most properties exhibited by biofilms are related with this particular matrix’s composition. It is mainly composed of water and contains structural and functional components, usually referred to as extracellular polymeric substances (EPS). Water is essential to embed all these compounds, to provide a vehicle for diffusion of nutrients to the inside and toxins to the outside, to maintain osmotic pressure and ensure microbe mobility [8]. The EPS are mainly soluble compounds such as proteins, polysaccharides, extracellular DNA (eDNA) and lipids derived from cell metabolism and cell lysis, as well as insoluble compounds as cellulose, pili, and flagella. This matrix serves as a house for the microorganisms providing them with a safe haven from external stimuli [20]. Accordingly, biofilms demonstrate many evolutionary advantages in comparison to the singular state such as cell-cell interactions, horizontal gene transfer, quorum sensing, metabolite exchange, protection under stress conditions (e.g., nutrient scarcity, extreme temperature and pH, shear forces), resistance to antimicrobial agents (e.g., antibiotics, disinfectants, antiseptics) and to host’s immune system response (e.g., antibodies, phagocytes) [3]. In fact, bacteria within biofilms are more tolerant than its planktonic equivalent since biofilm antimicrobial susceptibility can be 1000 times higher [27]. Biofilms usually form as an intrinsic defense mechanism to establish a favorable environment, preserve nutrients, and ensure their own survival [28]. It is relevant to mention that the chemical composition of the EPS matrix is not constant during biofilm development and is dependent on the environment conditons and cellular interactions therefore, biofilm properties might also vary with time [29, 19].

As mentioned, biofilms are mainly heterogenous and so, its cells arrange themselves according to social phenotypes [30]. Typically, biofilms present one of three main spatial organization types: microcolonies, co-aggregation and layered, as shown in Figure 2.1. In aggregated biofilms, distinct microcolonies of each species are formed on the surface (Figure 2.1A). This arrangement is observed when species exhibit antagonistic phenotypes and compete for nutrients [31, 23]. Oppositely, cells from different species can colonize the same area and prosper in a synergistic environment, forming mixed biofilms (Figure 2.1B) [30, 32]. Finally, a third organization can be adopted, either for cooperation or competition, where a layer of the dominant species is formed on top of the others (Figure 2.1C) [33].

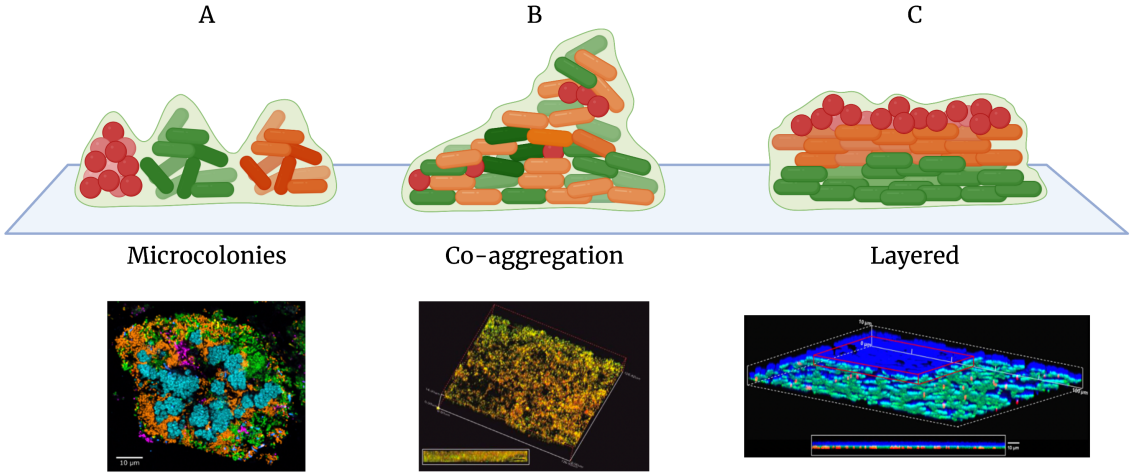

Figure 2.1: Commonly observed spatial distributions of bacterial cells within a biofilm: (A) separate microcolonies, (B) co-aggregation, (C) arrangement in layers. (Adapted from Barbosa et. al (2023) [3]). Created with BioRender.com

The preferred model for biofilm development is generally described by five major steps - initial attachment, surface colonization, formation of microcolonies, maturation and dispersal, as summarized in Figure 2.2A [4]. The initial contact of planktonic bacteria with a surface is the starting point for biofilm formation. At first, the attachment is reversible since the bacteria are solely relying on unspecific physio-chemical interactions (i.e., hydrophobic and electrostatic interactions, Van der Waals forces and protein bonding) for adhesion. Then, the microorganisms will start to colonize the surface by forming a monolayer by production of EPS. At this point, bacteria will use its appendages (i.e., flagellum and pili) and extracellular matrix proteins (i.e., collagen, fibrinogen and fibrinoctin) to bind to host components and become irreversibly attached [34]. This stage is also related to changes in phenotype such as increased and localized expression of adhesins and pili, hyperflagelation and cell elongation. Once establish a strong bacteria-surface interaction, the microorganisms will grow and proliferate. As the biofilm grows and matures, the cells develop and differentiate into specialized subpopulations, which can perform distinct functions and interact with each other in complex ways such as gene regulation and quorum sensing [35]. In the last stage, certain cells of the mature biofilm will disperse into the surrounding environment as planktonic cells, potentially initiating a new cycle of biofilm formation [36, 37]. It is important to emphasize that all described events are not single isolated occurrences that follow a linear path; in fact, distinct processes, potentially overlapping, will occur during biofilm development, but it is just a model, and as British statistician George Box said, “all models are wrong, but some are useful”. Specifically, this model falls short from reality because it lacks the representation of the diverse range of biofilm structures and phenotypes [3, 4]. In fact, a new broader approach has been presented by Sauer et. al (2022) [5]. The new model, despite being a work in progress, represents three basic events (aggregation, growth and disaggregation) that depict most of the different scenarios from biofilm development, independently of time and maturity, as shown in Figure 2.2B. This simpler model intends to be more inclusive, relieving some of the misconceptions regarding biofilm formation in the most diverse environments [5].

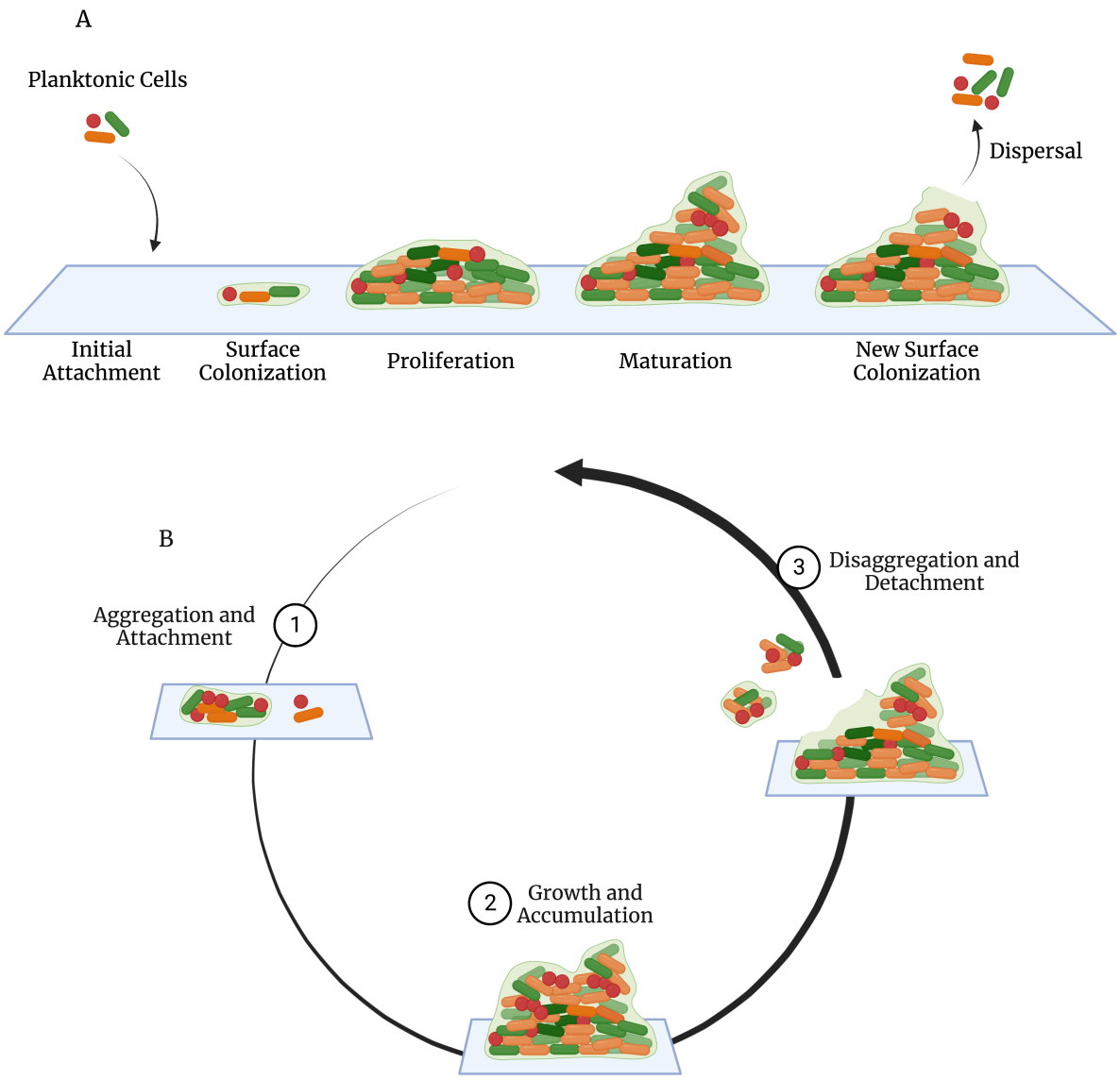

Figure 2.2: Conventional model of biofilm formation (A) (Adapted from Guzmán-Soto et. al (2021) [4]) and a more inclusive model (B) (Adapted from Sauer et. al (2022) [5]). Created with BioRender.com

As everything, biofilms have a good and bad side. Bioremediation, bioleaching, production of biofuels, clearance of oil spills, water and wastewater treatment are some of the many useful applications of this life form. On the opposite side, biofilms present many detrimental effects including biofouling, corrosion and numerous implications in fields such as the food industry and medicine (e.g., biofilm-associated infections) [33, 23]. The effects of bacterial biofilms in health will be further discussed.

2.2 Biofilms in Health

Biofilms are particularly concerning in the medical field as they provenly hinder the treatment of bacterial infections due to their distinctive discussed characteristics [1]. According to the World Health Organization (WHO), healthcare-associated (nosocomial) infections affect around 1.4 million people annually. Complementarily, the Centers for Disease Control and Prevention reports that around 70% of healthcare-related infections emerge from bacterial biofilms [38, 39]. Due to the significant impact of microbial biofilm infections, extensive research has been and continues to be conducted on the topic, aiming to enhance our knowledge on these infections and their lifestyle. This will be of particular importance to identify the microorganisms responsible and to sustain the development of innovative strategies to fight them. In fact, a diverse range of bacteria has been isolated from healthcare-related infections. *Enterococcus*

faecium (*E. faecium*), *Staphylococcus aureus* (*S. aureus*), *K. pneumoniae*, *Acinetobacter baumannii* (*A. baumannii*), *P. aeruginosa*, and *Enterobacter* spp., commonly referred to as ESKAPE pathogens, have been reported the main cause of nosocomial infections [40, 41].

Enterococcus spp. are Gram-positive facultative anaerobes that normally inhabit the gut of warm-blooded animals. More than 20 *Enterococcus* spp. are identified but the most clinically relevant are E. faecium and E. faecalis [40]. Studies have revealed that all enterococci exhibit decreased susceptibility to penicillin and ampicillin, as well as increased resistance to cephalosporins and semi-synthetic penicillins, due to the expression of low-affinity penicillin-binding proteins [42].

S. aureus is a Gram-positive, metabolically flexible, non-fastidious bacteria that is part of the normal skin flora of animals. This species has also been reported as resistant to many clinically relevant antibiotics (e.g., penicillin, clindamycin) [40, 43].

Moreover, *K. pneumoniae* is a Gram-negative facultative anaerobe that belongs to the Enterobacteriaceae family. It is also a non-fastidious bacteria and is usually found in the respiratory and gastrointestinal tract of animals [40]. Throughout the years, multiple-drug resistance (MDR) and carbapenem-resistant *K. pneumoniae* have arised, which constitutes a serious health issue since carbapenems are the preferred antibiotic when dealing with critical MDR bacterial infections [44]. *Klebsiella* infections are related with high rates of mortality, especially amongst immunodeficient patients [45].

A. baumannii is a Gram-negative non-fermentative bacteria commonly found in nature (e.g., soils, water) and hospital settings. Similarly to *K. pneumoniae* the respiratory and urinary tracts are some of the affected sites of its infections [40] and, strains from this species began displaying resistance to carbapenems, which led it to be classified as MDR [46, 45].

P. aeruginosa is a Gram-negative facultative anaerobe habitant of the normal gut flora of animals. Infections from this pathogen occur mainly from an exogenous source and affect mostly immunocompromised patients [40]. Many *P. aeruginosa* strains exhibit an intrinsically lower susceptibility to several antibacterial agents, as well as a propensity to develop resistance during the treatment. More specifically, strains of *P. aeruginosa* may show resistance to many antibiotics including aminoglycosides, quinolones and β-lactams like carbapenems [47].

Enterobacter spp. are Gram-negative non-fastidious bacteria that can cause opportunistic infections in immunocompromised patients and contain a wide range of antibiotic resistance mechanisms [40]. These species are generally considered resistant to penicillin and many cephalosporins due to the production of a chromosomal β-lactamase exhibiting cephalosporinase activity [48].

The urgency of the MDR microbes was made unequivocal when, in 2017, the WHO published the first ever list of "antibiotic-resistant bacteria to guide research, discovery and development of new antibiotics", in which *A baumannii*, *P. aeruginosa* and Enterobacteriaceae spp. made the top 3 of critical priority [49].

As previously mentioned, biofilms have the ability to perform horizontal gene transfer (HGT), which simply means that cells are capable of exchanging resistance genes within themselves, through plasmid transfer, viral delivery or free DNA. Due to this competence, bacteria in a polymicrobial biofilm might gain resistance to certain antibiotics, becoming MDR, which is a very relevant issue in nowadays medicine practice [50].

Essentially, biofilms can be accountable for infections associated with the use of medical devices (e. g., urinary and central venous catheters, endotracheal tubes and orthopedic prostheses) and actual colonization of human tissues (e. g., chronic wounds (CW), prostatitis and CF) [51]. As an example, CW such as arterial or leg ulcers, are the ones that fail to heal through the normal stages within the expected time and they are usually caused by internal factors that can be associated with diseases like diabetes or

immune deficiency diseases. CW and biofilms (particularly from ESKAPE bacteria) are tightly connected since these are a major contributing factor for their persistence [52].

Another example of the nefast impact of biofilms in the human body occurs in CF, which is an autosomal recessive disease caused by a mutation in the cystic fibrosis transmembrane conductance regulatory (CFTR) gene. This gene encodes the CFTR protein which is essential to the chloride channel whose function is to pump ions in and out of the cell. The complications and severity of CF varies widely amongst patients, but most may exhibit symptoms including pancreatic insufficiency and chronic lung infections. CF is associated with the excessive accumulation of viscous, dehydrated mucus over lung epithelial cells that provide a niche for bacterial colonization. These conditions transform the patients' airways into a heterogenous microenvironment with gradients of oxygen, nutrients, pH and antibiotics which contributes greatly to the colonization and proliferation of phylogenetically diverse microbes [53, 54, 55, 2, 56].

CF communities of organisms may include bacteria, fungi and viruses, with the first being more frequent. In fact, mucus samples from the lungs of CF patients consistently reveal the presence of *P. aeruginosa* and *S. aureus*, making them the most relevant microorganisms in CF. Another prevalent pathogen in CF, that also belongs to the ESKAPE bacteria, is *K. pneumoniae* [57, 58, 59]. As microbiological diagnostic tools evolved, many other microorganisms have been appointed as atypical CF pathogens (e.g., *Dolosigranulum pigrum*, *Inquilinus limosus*, *Candida albicans*) [55, 60, 2].

Since its first description in 1938, CF patients' life expectancy has increased in about ten times which is a great achievement that we owe to the refinement of diagnosis techniques and treatment options [61]. An interesting observation is that CF airway microbiome changes throughout disease course. Up until a decade of age, the microbial diversity in the lungs of CF patients is high, which is lost with age. In fact, diversity has been a marker of lung function in CF, since stable respiratory function has been related to high diversity and the opposite with decreased diversity. This decline is usually associated with the dominance establishment from a specific pathogen, usually *P. aeruginosa* [62]. In 2008, a study was able to discriminate the different pathogens present in sputa samples from different age patients, recurring to molecular techniques like 16S rDNA sequencing. In children a larger variety of species was identified with the two most prevalent being *Stenotrophomonas maltophilia* and *Streptococcus pneumoniae*, besides *S. aureus*. In adults, only three species were identified, *S. aureus*, *P. aeruginosa* and *K. pneumoniae* [60], predictably, these are ESKAPE pathogens. A more recent study, aiming to characterize the phylogenetic diversity of the CF microbiota of different age patients, reported that *S. aureus* was more common in the pediatric population and with age progression *P. aeruginosa* was the prevalent pathogen [63]. In fact, *S. aureus* is generally recognized as the initial colonizer of the CF airways, causing infections that instigate changes in the lungs allowing for other pathogens infections (e.g., *P. aeruginosa*) [64]. Therefore, this type of microbial discrimination and understanding of their dynamics is essential to fight the infection or, at least, reduce its complications.

One of the main goals of CF treatment is controlling lung infections with antibiotics, generally in their aerosolized form to act *in situ* [65]. Despite, antibiotic therapy is not always effective on bacterial infections termination, in fact, intensive antibiotic application to chronic *P. aeruginosa* airway infections is rarely, if ever, permanently eradicated, specifically in CF patients where *P. aeruginosa* strains with resistance to β-lactam antibiotics are frequently found [66, 67, 47]. Studies have shown that biofilms of *P. aeruginosa* respond to β-lactam antibiotics by increasing the production of β-lactamase [68]. Apart from these antibiotics, *P. aeruginosa* exhibits resistance to many others throughout all classes, more specifically, it presents resistance to the most clinically relevant antibiotics (e.g., tobramycin, gentamicin, levofloxacin) [69].

In summary, bacterial biofilms such as those associated with CF have serious impacts on human health, making patients fight lifelong infections [70] and increasing the burden on the healthcare system, which is why it is necessary to keep devoting efforts into developing new and more accurate techniques to their study.

2.3 Platforms and Methods to Study Biofilms

2.3.1 Platforms for Biofilm Formation

Regarding the study of biofilms, it is possible to discriminate between two important stages: the culture of the biofilm and the analysis of the biofilm. The culture of biofilms is an arduous task since one must ensure that the characteristics of a natural environment are being faithfully recreated. Nowadays, some in vitro, *ex vivo* and *in vivo* models are available for this purpose [12]. The requirements and aim of each experiment should be considered when choosing any of these models [71].

In vitro biofilm models have been intensely implemented to enlighten us on some topics including biofilm formation, adhesion and to investigate the efficacy of new antibiotics against microbial infections. The main advantages of *in vitro* models comprise its low cost, simplicity and high-throughput. Although, it is generally accepted that these models do not accurately replicate biofilm characteristics such as nutrient and metabolite gradients [72]. According to the literature, in vitro models can be generally classified as closed or open, whether relating to a static or dynamic model, respectively [73].

More specifically, in closed models the bacteria are let to grow with limited nutrients and aeration, since there is no fluid flow. Microtiter plates (6, 12, 24, 96-well plates), Calgary Biofilm Device (CBD) and Biofilm Ring Test (BRT) are some of the most used *in vitro* systems for artificial biofilm growth. In microtiter plates, the biofilm grows on the bottom and walls of each well. These are usually made of polystyrene, polypropylene, cyclic olefin polymer and cyclic olefin copolymer [74], which are synthetic materials that evidently fail to mimic natural environments. Depending on the assay, a coupon of a specific material being investigated might be added to the well to evaluate biofilm development on that surface more accurately [75]. This platform has commonly been applied to assess biofilm formation capacity on specific surfaces and to high-throughput screening of various conditions (e.g., antibiotic susceptibility, temperature, pH, shear stress, O_2 and CO_2 concentration) [76]. Nevertheless, these models exhibit low reproducibility amongst assays and do not allow direct observation of the spatial location of bacteria within the biofilm without disruption [72, 3]. Microtiter plates were taken a step further to address these concerns by the creation of the CBD, which fundamentally is a 96-well microtiter plate with 96-prong replicator with plastic pegs to which cells will adhere. The CBD is especially useful to determine antimicrobial susceptibility and for microscopic visualization of biofilms adhered to the pegs [12, 77]. The BRT is another variant of microtiter plates in which magnetic microbeads are involved to indirectly assess biofilm growth. Briefly, if the biofilm is present, the beads become trapped, losing mobility, and do not exhibit a spot. On the other hand, in the absence of the biofilm, the beads will exhibit a visible spot when magnetized [78].

In its turn, open or dynamic models refer to flow-based continuous culturing that create a relatively more similar natural environment. These systems assure constant nutrient supply during the experiment, enabling long-term analysis of biofilm formation kinetics, since nutrients and wastes are partially replaced and removed, respectively. Regardless, open models generally involve a slower, more focused analysis, also being more resource-demanding and therefore expensive. The Robbins Device/Modified Robbins Device, CDC Biofilm Reactor and Drip Flow Biofilm Reactor (DFBR) Device are some examples of the most commonly used open loop systems [12, 72].

The Robbins Device/Modified Robbins Device is a tower equipped with coupons with parallel alignment with the fluid flow, and where biofilms form. This platform is used to assess biofilm formation on different surfaces under different hydrodynamic conditions. Some advantages of this device are the large amount of produced biomass, the enabling of periodical sampling and the unsupervised running. Its complex setup is a disadvantage alongside the limited *in situ* visualization and the necessary destruction of biofilm for the most analysis [71].

The CDC biofilm reactor comprises a vessel with mounted coupon holders in which a liquid growth media or biocide can circulate while a magnetic stir bar ensures mixing. Biofilm development under the effect of shear stress is one of the applications of this platform. Similarly, to the Robbins Device, this apparatus allows biofilm growth on different surfaces and allows for aseptically sampling of the biofilm. It

has been broadly used to study biofilms due to its robustness and high reproducibility. On the other hand, it is an expensive material, and the geometry of the coupons is limited to the design of the coupon holders [12, 79].

Lastly, the DFBR consists of parallel tilted chambers with vented lids equipped with a coupon each where the biofilm forms. This device requires a small setup space, easy operation and test of various surface materials. Nevertheless, it presents some limitations regarding the heterogeneity of biofilms developed on the coupons due to flow hydrodynamics, disparity to real industrial circumstances and limited number of samples tested [12, 80].

Overall, *in vitro* models share one major limitation that is their inability to provide for a biotic surface for microbial biofilm formation. To account for this limitation, *ex vivo* models have been considered. *Ex vivo* models concern the culture of bacterial species in the presence of animal/human tissues or organs (e.g., skin, cardiac valves, lung, dental and mucosal sections) outside of an organism using *in vitro* platforms. Some of the advantages of *ex vivo* models include the use of well-preserved 3D-structured tissues, the controlled and reproducible culture conditions, the possibility of real-time monitoring of biofilm kinetics using optical coherence tomography and the use of tissues extracted from animals used in meat industry, reducing ethical impairments [81]. Still, *ex vivo* models fall short from *in vivo* conditions since they cannot replicate the host's immune system response to bacterial colonization of tissues, they may not exhibit the competing microbiota on the tissues, and they do not replicate fluid flow experienced *in vivo* [73].

Simple, intuitive, hybrid models that combine features of the others, decreasing the differences from *in vivo* conditions are being developed. For instance, microtiter plates combined with novel substrates that mimic the microenvironments in which microorganisms are found in nature were developed by Bac^{3}Gel [11]. This startup is pioneering the development of advanced substrates that combine a 3D architecture with oxygen and nutrient gradients that replicate key features of the human mucus, where vast microbial communities reside [82]. In fact, Bac^{3}Gel has been able to reproduce the way in which pathogens organize themselves in the human body and show resistance to microbial treatments that are closer to what is reported in the literature. This company has available many models simulating various human mucus, including the pregnancy cervicovaginal mucus, the large intestinal mucus, the pathological lung mucus, amongst many others. Therefore, the main advantage of this novel models is its simplicity allied to a better replication of human body microenvironments [11].

2.3.2 Methods for Analysis and Characterization

After ensuring reproducible biofilm growth, it is important to select the most adequate method for analysis. Depending on the experiment's aim (e.g., measurement of cell viability, cellular biomass, metabolic activity and biofilm biomass), there are many molecular and non-molecular methods available. The most commonly used methods for different assessments will be discussed further.

Cell cultivability of biofilms is commonly assessed by determination of colony forming units (CFU) on agar or selective media. It is a standard procedure in which the biofilm is disrupted, and a series of dilutions are plated in a favorable universal medium or specific selective media, followed by incubation and cell counting. This method does not require highly specialized equipment which constitutes an advantage; however, it can be time consuming, it may not be representative of the initial biofilm population and may neglect viable but non-culturable (VBNC) cells [12, 83].

In contrast, flow cytometry (FCM) is a more automated route to cell quantification since its principle is based on light scattering and fluorescence emission of a fluorescent-labelled probe, as cells suspended in an isotonic buffer flow through a laser beam. Limitations of FCM are the requirement of fresh samples and the need of cells in suspension. Nevertheless, this technique grants fast, quantitative, multiparametric assessment of cells [84, 85].

Additionally, viability quantitative polymerase chain reaction (v-qPCR) has been appointed as an alternative technique for estimation of cell viability. However, v-qPCR detects and quantifies the total RNA of a sample, which implies that RNA proceeding from eDNA will also be quantified [12, 86].

Physical methods such as the measurement of dry or wet biomass can also be useful to quantify total biofilm biomass. This is a straightforward principle that states that the difference between a dried slide with the biofilm and the dried slide prior to biofilm development equals to the total mass of the biofilm. Limitations of physical methods are the lack of sensitivity and time consumption [12].

Additionally, chemical methods rely on the binding and adsorption abilities of dyes or fluorochromes to biofilm components [12]. Biofilm physiology has been studied by colorimetric levels, whose basic principle is the assessment of cellular metabolic activity of a specific substrate with a colored product, passive of being measured by spectrophotometry. One of the most frequently used microtiter assays for quantification of biofilm biomass is Crystal Violet staining (CV). The compound that gives the name to the technique is crystal violet and it stains all cells (i.e., alive or dead), as well as EPS matrix components, which is why it is a reliable approach to estimate total biofilm biomass. Additionally, CV is a high throughput, versatile technique capable of being implemented in not only bacterial cells but also eukaryotic cells like fungi and yeasts. All CV protocols must be carefully performed since it comprises many washing steps and therefore can lead to biomass loss [12, 87].

The resazurin assay is also a commonly used method for biofilm quantification. Resazurin is a redox indicator that in its oxidized form is non-fluorescent blue/purple and when reduced by metabolically active cells becomes highly fluorescent pink; therefore, the number of viable cells can be obtained in relation to the amount of fluorescence. This is a low-cost technique that allows visual monitorization of metabolic activity by spectrophotometry or spectrofluorometry in a relatively quick time period [88, 89].

Other molecular techniques generally supply a broader range of information besides cell quantification such as genetic diversity in the biofilm, DNA/RNA/protein quantification and gene expression monitoring. Some of them are next-generation sequencing (NGS), quantitative reverse transcription polymerase chain reaction (RT-qPCR), RNA sequencing (RNAseq) and microarrays [3]. DNA sequencing technologies, such as NGS, have been implemented to isolate the total DNA of a sample to gather information regarding the genetic diversity, species composition, evolution and environment interactions of natural biofilms [90]. RT-qPCR is a quantitative assay based on the detection of a fluorescence labelled probe, previously attached to the gene of interest, during a PCR. It is a valuable technique because, unlike any other, provides real-time gene expression monitoring with the downside of only targeting one gene at a time [91]. In its turn, microarrays allow simultaneous assessment of multiple genes expression levels, which can be useful to identify microbes within a biofilm. Finally, RNAseq is a powerful tool to analyze and quantify RNA molecules in a biological sample, providing a comprehensive view of the transcriptome [92]. All described methods share one common limitation that is the requirement of sample destruction, hence ruling out the possibility of *in situ* observation of the biofilm. In fact, spatial organization/location of cells and components (i.e., genes) of a biofilm is one of the most relevant recent advances for understanding biofilm dynamics [93].

Nowadays, microscopy methods such as fluorescence and CLSM have emerged as some of the most powerful tools to study biofilms. From them, it is possible to quantify biofilm biomass, discriminate microorganisms and their combination may allow for the visualization of cell distribution within a biofilm [3].

Fluorescence microscopy uses filters that allow for the optical discrimination of different fluorescently labelled components of the sample [94]. As expected, sample preparation requires time and resources, since sample components (e.g., biofilm cells) must be fluorescently labelled. The strength of fluorescence imaging relies on the fluorescent markers used and the specificity with which cellular structures can be labelled [95]. One of the most used fluorescent markers is 4',6-diamidino-2-phenylindole (DAPI), which binds strongly to adenine-thymine regions in DNA of cells, either dead or alive, which will appear with a strong blue color under fluorescence microscopy. It is commonly used as a counterstain since it allows for

the visualization of all the cells in the sample [96]. The LIVE/DEAD assay is another example of fluorescence imaging that relates to the visualization of bacteria through fluorescence microscopy and, additionally, allows the discrimination of live and dead cells. In this assay, a combination of SYTO9 and propidium iodide (PI) is used to label cells and it will exhibit different colors according to the membrane integrity (cells with intact and compromised membranes will appear green and red, respectively) [3]. Both fluorescent markers are non-specific, so bacterial strains cannot be distinguished within a sample. A way of overcoming this limitation is resorting to recombinant DNA techniques. In this approach, the gene encoding a fluorescent protein (e.g., green fluorescent protein (GFP), mCherry) might be inserted in an expression vector and introduced in the selected bacteria strain. Upon fluorescence analysis, these bacteria will exhibit the fluorescent protein's color. This is a valuable technique regarding identification and location of microbes within biofilms; however, it requires genetic modifications of the species involved, which is a limitation because it requires complex sample manipulation and it will not be feasible for analysis of naturally occurring biofilms [3]. To surpass these limitations, FISH emerged.

These fluorescence labelling techniques can be combined with CLSM enabling a three-dimensional visualization of biofilms [23].

2.4 Fluorescence *in situ* Hybridization (FISH) for the detection and *in situ* visualization of microorganisms

In situ hybridization (ISH), is a classical technique that was firstly introduced in 1969 by John et al. and Buongiorno-Nardelli and Amaldi for rDNA detection in the frog Xenopus and paraffin-embedded tissues [97, 98], followed by its application to localize chromosomes in mammalian cells. To this point, labelling was exclusively performed by employment of radioactive isotopes which presented many disadvantages such as long exposure times (up to weeks) and low spatial resolution [99]. These limitations significantly highlighted the need for new labelling molecules. The first non-radioisotopic probes emerged in the 70s, and a decade later, the first direct fluorescent detection was performed recurring to a fluorochrome labelled RNA probe by Bauman et. al (1980) [100]. In fact, this study laid ground for the synthesis of novel fluorescent probes for FISH.

Since its development, FISH suffered great improvements of probe-labelling techniques and specific probe design strategies increasing its sensitivity and allowing its establishment as a reliable tool for detection and spatial discrimination of nucleic acids in their cellular environment [101].

In its core, FISH is a "cytogenetic technique allowing for high-resolution detection, quantification and localization of nucleic acid targets inside cells or tissues" [101]. The fact that this technique allows for the discrimination and visualization of specific targets (i.e., DNA, RNA) inside cells is a major contribution factor to why it is employed in many fields. Medical applications of FISH are one of the most relevant since these methods can be applied to disease diagnosis [102]. Probes targeting chromosomes or chromosomal regions have allowed for the identification of many diseases such as CF, Duchenne's muscular dystrophy and leukemia [103]. Additionally, FISH can also be employed to report on abnormal gene amplifications associated with tumors [104, 105]. It also plays a significant role in microbial identification not only in the medical field, but also in nature and industry [106].

Regarding cell identification, the basic principle of FISH concerns probe targeting of 16S/23S rRNA (for Bacteria or Archaea) or 18S/28S rRNA (for Eukarya) sequences [107]. The rRNA was chosen as the preferred target molecule due to its high copy number in cells and their use as phylogenetic markers [16]. In fact, a single cell like *Escherichia coli* (*E. coli*) can exhibit rRNA numbers between 10^4 to 10^5. This way, it is simple to understand that fluorescence intensity is a result of rRNA copies and therefore can vary greatly depending on the species and growth phase. Being an almost quinquagenarian technique, the FISH protocol is now well-established and mainly comprises four steps: fixation/permeabilization, hybridization, washing, visualization/analysis [22, 6], as shown in Figure 2.3.

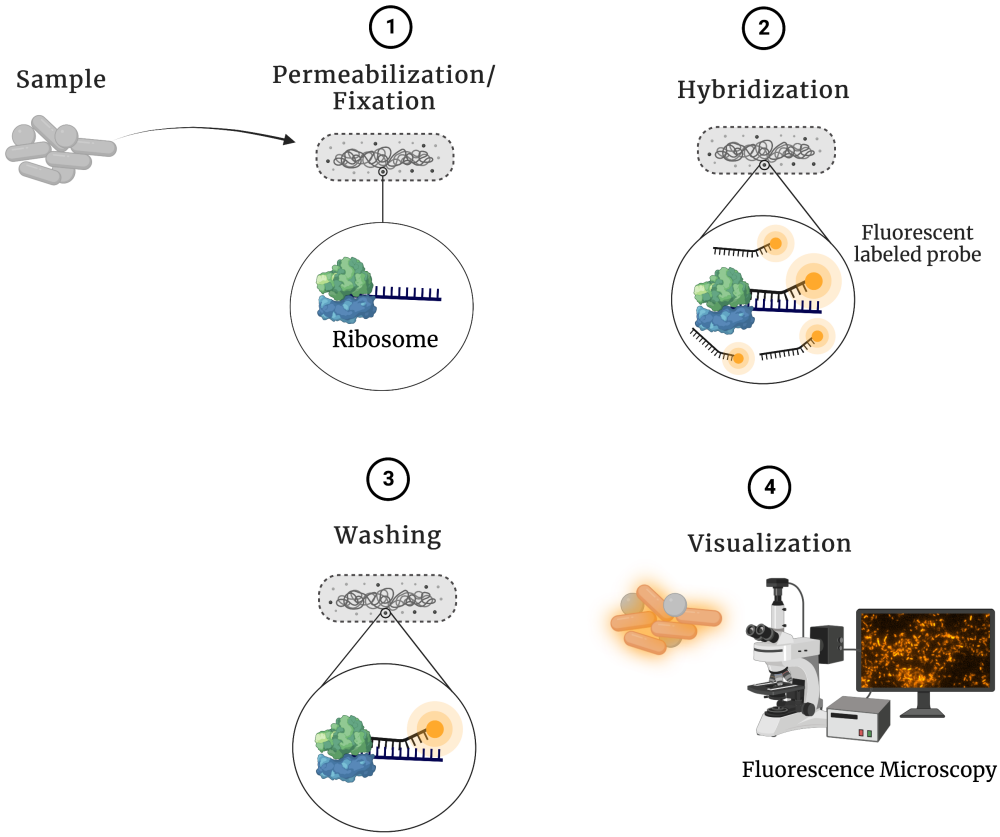

Figure 2.3: Traditional FISH protocol. The biofilm sample is chemically permeabilized and fixed (1), followed by hybridization (2) with a fluorescently labelled probe. To remove unbound probes so imaging is not compromised, a washing step (3) is carried out before fluorescence microscopy (4). (Adapted from Barbosa et. al (2023) [3]). Created with BioRender.com

For the first step (Figure 2.3, Step 1), a set of chemical compounds (i.e., paraformaldehyde and ethanol) are applied to the sample to induce fixation which basically ensures the preservation of nucleic acid integrity and cell morphology and the permeabilization of the membrane, which is essential to facilitate probe penetration [108]. For Gram-positive bacteria, a pre-treatment (with enzymes, detergents, solvents, hydrochloric acid) might be necessary, due to its cell wall nature [109]. More specifically, Gram-negative bacteria present a thin peptidoglycan cell wall surrounded by an outer membrane, whilst Gram-positive bacteria lack the outer membrane but are protected by a thick peptidoglycan wall [110]. The following step is hybridization (Figure 2.3, Step 2), where the sequence-specific probe and the sample are incubated under specific conditions (temperature, time, pH, ionic strength, probe concentration, denaturing agent concentration) that will determine the hybridization efficiency. This step must be optimized for each individual probe considering the microorganism(s) used and the probe's characteristics [107, 111]. Naturally, a washing step (Figure 2.3, Step 3) is performed after removing any unbound probe so that it does not compromise further imaging quality [112, 29]. At this point, the sample is set to undergo fluorescence microscopy (Figure 2.3, Step 4). Note that all these steps might be conducted without sample/biofilm destruction and therefore, this technique can be combined with CLSM for providing valuable information on spatial organization of the biofilm (Figure 2.1).

Many variants of FISH have emerged during the years providing robustness to the traditional approach and offering different information for different aims including the improvement of standard FISH sensitivity (catalyzed reporter deposition, CARD-FISH), the identification of microbes within a natural sample through the presence genes (Gene-FISH), the assessment of metabolic activity of microbes (microautoradiography, MAR-FISH) amongst others [15]. Most of these variants share one common limitation which is the reduced number of possible distinguishable microbes. CLASI-FISH then emerged as a complex technique that allows for the discrimination of a greater number of microorganisms within a single FISH assay. Its principle is based on the hybridization of a species with at least two versions of the

probe, each conjugated to a distinct fluorochrome, allowing for the detection of up to 120 different targets [113]. Although, some cells with low ribosome content may be neglected since the probes are competing for the same site and therefore fluorescence intensity might be lower. Additionally, the great number of probes required means that extended efforts must be dedicated to probe design, to ensure successful hybridization of all probes under the same hybridization conditions [114]. To eliminate this competition, it is also possible to use different probes with different fluorochromes, although, the optimization complexity becomes much greater due to the higher number of different probes that must hybridize an organism under the same hybridization conditions and present similar efficiency [115].

Due to its relevance for this particular work, NAM-FISH will be explored further.

2.4.1 NAM-FISH

Even though FISH was soon established as a very valuable tool, there is always room for improvements. At some point, it was recognized that the employment of DNA/RNA probes constituted a limitation regarding specificity and stability. The EPS matrix of biofilms is composed of many negatively charged molecules that hinder the diffusion of DNA probes and, to overcome these natural nucleic acid limitations, nucleic acid mimics (NAMs) started being developed and used as probes in FISH [116].

NAMs are not more than chemically modified nucleic acids on the nucleobase, the sugar ring or the phosphodiester backbone, that still stay true to the Watson-Crick base-pairing rules. Currently, different NAMs are available with the most prevalent being Peptide Nucleic Acid (PNA), Locked Nucleic Acid (LNA) and 2'OMethyl-RNA (2'OMe), which structures can be observed in Figure 2.4.

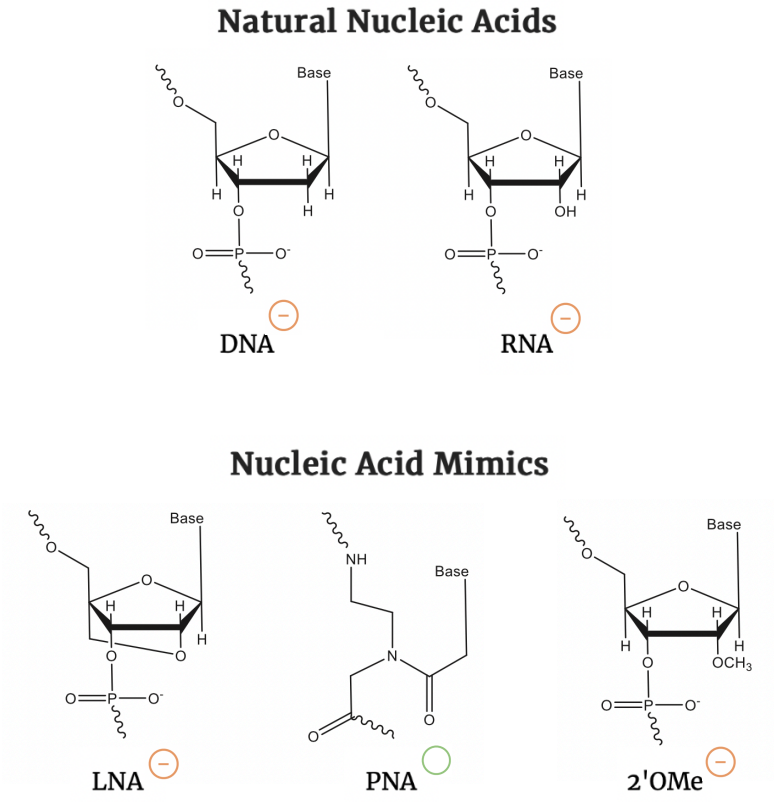

Figure 2.4: Chemical structure of the natural nucleic acids (DNA and RNA) and the NAMs (LNA PNA, 2'OMe) described in this work. Nucleic acids with negative charge (DNA, RNA, LNA and 2'OMe) are labelled in orange and nucleic acids with neutral charge (PNA) are labelled green. (Adapted from Oliveira et. al (2021) and M. Nacher-Vasquez et. al (2022) [6, 7])

In 1991, PNA was published as the first synthetic DNA analogue, with the distinctive feature of a neutral peptide backbone, rather than the negatively charged sugar backbone from DNA. This characteristic diminished the probe-target repulsive electrostatic interactions resulting in a stronger probe-target sequence bond. This feature also results in a higher melting temperature (Tm), which physically allows the use of shorter probes (15 bp) conferring high stability and specificity. The neutral charge gives an apolar configuration to PNA which increases its penetration capacity through the EPS matrix of biofilms and cell membrane [6, 7].

In turn, in 1997 the first LNA was synthesized and reported as an RNA analogue with a ribonucleoside between the 2'-oxygen and the 4'-carbon with a methylene unit. LNA has many reported advantages, including higher affinity towards DNA and RNA targets, higher biostability (resistance to nuclease degradation), better signal-to-noise ratio and better sensitivity and specificity [117, 6]. Additionally, LNA incorporation in DNA duplexes has revealed increased thermal stability, with increase of 1ºC to 8ºC per LNA nucleotide [6].

Similarly, 2'OMe is also an RNA mimic with the peculiarity of a C3'-endofuranose ring conformation, with high affinity for RNA targets. It has been reported that the implementation of LNA/2'-OMe probes delivers finer detection of rRNA and identification/location of microbes and allows for more probe design flexibility [118, 119].

Contrary to PNA, LNA/2'OMe holds a negative charge which could constitute a great disadvantage since hybridization requires that these probes penetrate through the biofilm matrix, which is mainly composed of eDNA and other proteins that are also negatively charged. This means that the electrostatic repulsive forces between the probe and the matrix compounds could restrain probe diffusion and therefore compromise hybridization [7]. This concern was discarded as Azevedo et. al (2015) reported that LNA/2'OMe probes did not face diffusion restrictions when penetrating the biofilm matrix, successfully staining the biofilm and exhibiting a strong fluorescent signal. Due to all these characteristics, LNA/2'-OMe probes are typically employed successfully in multiplex detection essays [120].

In addition, NAM-FISH still presents relevant drawbacks such as low number of distinguishable targets in a single essay. In fact, the number of fluorochromes passive of being detected by epifluorescence microscopy is limited to 3/4 due to the wide band spectrum of available filters [3]. To address this issue, Azevedo et. al (2022) recently combined LNA with 2'OMe probes, which allowed for the design of species-specific probes with similar hybridization conditions (overcoming CLASI-FISH drawback) prone to being used in multiplex assays, and spectral imaging that allowed for unambiguous discrimination of the microorganisms [120]. The unquestionable value of NAMs for multiplex assays is making LNA/2'OMe-FISH the preferred technique for microbe detection [7]

3 Materials and Methods

3.1 Universal-Bac^{3}Gel Properties

Universal-Bac^{3}Gel (Figure 3.1) mostly consists of a polysaccharidic mesh, containing 0.2% (wt/vol) Ca^{2+} ions, 0.71% (wt/vol) NaCl, and it is produced in Mueller Hinton Broth (MHB) [Sigma Aldrich, Spain]. Universal-Bac^{3}Gel was produced exploiting the licensed technology of Bac^{3}Gel, Lda, Portugal[34] that enables the generation of 3D structures with spatial gradients.

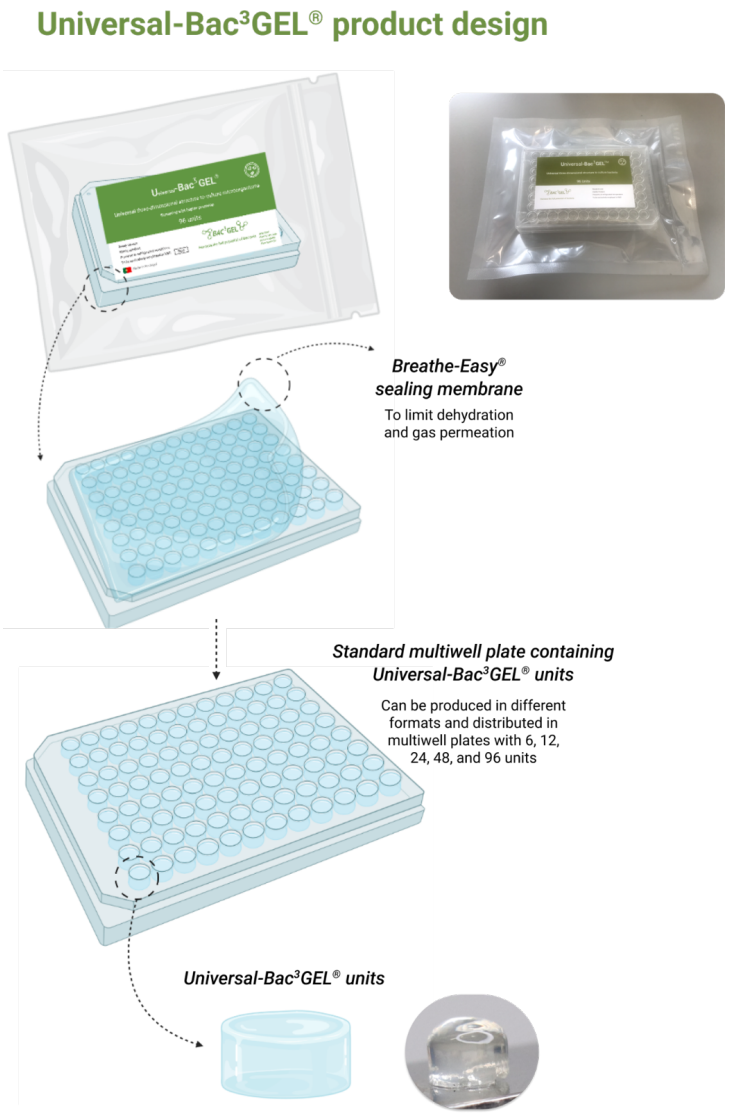

Figure 3.1: Product design of Universal-Bac^{3}Gel.

3.2 Rheological Characterization of Universal-Bac^{3}Gel

Viscoelastic properties of Universal-Bac^{3}Gel were assessed as described by Pacheco et. al (2023) [11]. An Anton Paar MCR501 Rheometer [Austria] with a 25 mm diameter plate geometry (serial number 7810/79044) was employed for the evaluation, at 25ºC. Strain sweep analyses using a strain logarithmic ramp varying from 0.1 to 1000% at a frequency of 1Hz were used to determine the linear viscoelastic region (LVR). Subsequently, oscillatory frequency sweeps were conducted to evaluate both storage/elastic, G', and loss/viscous, G'', moduli, as well as complex shear modulus, G^*, at 1.0% (within linear regime) with frequencies changing logarithmically in the 0.1–10 Hz range.

The oscillatory test is useful to identify whether the material behaves as shear-thinning or shear-thickening if the viscosity increases or decreases with respect to the frequency of oscillation. It allows identification of the behaviour of the viscoelastic properties, through the monitoring of the viscoelastic parameters, G'and G'', at different oscillation frequencies with a set strain. The total resistance of the material to a shear deformation is often described as G^*, which is a function of both moduli (Equation 3.1) [121].

$$G^* = G' + iG'' \tag{3.1}$$

$$G' = G^* \cos\delta \tag{3.2}$$

$$G'' = G^* \sin\delta \tag{3.3}$$

- δ is the phase angle between stress application and stress response. In a perfectly elastic solid, this angle corresponds to 0º. As it approximates to 90º, it means the material has a closer behavior to a fluid.

The LVR comprises the region where G' and G'' are independent of strain amplitude. Through the length of the LVR it is possible to conclude about the elastic character of the hydrogel [122].

3.3 Bacterial Strains and Culture Conditions

As a case study, *P. aeruginosa* PAO1 and *K. pneumoniae* ATCC 43816 were selected. Both species were streak plated from a frozen glycerol stock (-80ºC) onto Tryptic Soy Agar (TSA) [3% (wt/vol) tryptic soy broth; Sigma-Aldrich, Germany and 1.5% (wt/vol) agar; VWR Chemicals, Italy] and subsequently incubated overnight at 37ºC. Colonies isolated from each species were inoculated separately in 75 mL of MHB [Sigma-Aldrich, Spain] and then incubated at 37ºC, with agitation (120 rpm), overnight (16-18h). Afterwards, 10 mL of each inoculum were centrifuged at 4000 rpm for 10 min. The remaining pellets were washed twice with saline solution 0.85% (v/v) [NaCl; Sigma-Aldrich, Denmark]. The resuspended inocula were diluted in MHB to a concentration of 10^6 cells/mL as determined by comparing the optical density at 620 nm of the sample with a standard curve relating OD_{620} to bacterial count by using an UV-VIS spectrophotometer [LLG-uniSPEC 2]. The inocula prepared were then used for single- and dual-species biofilm formation as previously described by Azevedo et al. (2014) [22].

3.4 LNA/2'OMe-FISH in Glass Slide

In a preliminary test, the standard FISH protocol was tested on glass slides as described by Oliveira et. al (2021), in order to verify the LNA/2'OMe probes performance [6]. Two different LNA/2'OMe probes were used according to Table 3.1; a species-specific LNA/2'OMe probe was used to label *P. aeruginosa* PAO1 and a universal LNA/2'OMe Eubacteria probe (EUB338) was used to label *K. pneumoniae* ATCC 43816. As stated, EUB338 is a universal probe which means that it is able to hybridize all microbial species. Hence, the detection of *K. pneumoniae* when co-cultured with *P. aeruginosa* in dual-species biofilms was calculated as the difference of total cells labelled with EUB338 and total cells labelled with *P. aeruginosa* species-specific probe.

Table 3.1: Characteristics of the LNA/2'OMe probes used in the present study for hybridization of *P. aeruginosa* and *K. pneumoniae*, such as the rRNA subunit binding site, its sequence, the attached fluorochrome and reference. LNA and 2'OMe-RNA nucleotide monomers are represented in lowercase and capital letters, respectively.

Target	rRNA subunit	LNA/2'OMe probe sequence (5'-3')	Fluorochrome	Reference
P. aeruginosa	23S	cTTgAAaccCCgGAt	ATTO 550	Azevedo et. al (2022) [120]
Eubacteria	16S	UgCCtCCcGUaGGa	Alexa Fluor 488	

Briefly, biomass from the streak plated TSA was diluted in sterile distilled water to a concentration of 10^8 cells/mL. A volume of 20 µL from this suspension was placed in 14 mm well slides [Marienfeld, Lauda-Königshofen, Germany] and let heat dry in the incubator at 62ºC. Next, the smear was covered with 4% (v/v) paraformaldehyde [Sigma-Aldrich, Germany] for 10 min. This step was repeated with 50% (v/v) ethanol and then followed hybridization. For the hybridization, 40 µL of hybridization solution containing 200 nM of each LNA/2'OMe probe, 50 mM Tris-HCl (pH 7.5) [Roche Diagnostics, Germany], 2 M Urea [Merck, Germany] and 4 M NaCl [Sigma-Aldrich, Denmark] were added to the wells. The same volume of hybridization solution (without probe) was placed on another well to act as negative control. The slide was then incubated at 62ºC for 60 min. Simultaneously, a coplin jar filled with washing solution (5 mM Tris-Base [Fischer Scientific, USA], 15 mM NaCl [Sigma-Aldrich, Denmark], 1% Triton X [Sigma-Aldrich, USA] at pH 10) was also incubated. Afterwards, the slide was immersed in the heated washing solution and let incubate for 30 min at the same hybridization temperature. Finally, the slide was set to air dry in dark conditions and then was ready for microscopy analysis as described below.

3.5 Bacterial Colonization within Universal-Bac^{3}Gel

At an early stage, single-species biofilms were cultured in Universal-Bac^{3}Gel 96-well plates, to study the ability of each bacterium to form biofilms. For this purpose, a volume of 100 µL (equal to the hydrogel volume in the well) of each bacterial inoculum was transferred into each well in triplicate. The plates were then parafilmed and incubated during 24h and 48h, at 37ºC, under static conditions. Additionally, 100 µL of MHB was added to a distant well to assess medium sterility. For the 48h biofilm, fresh MHB was added at the 24h milestone after careful removal of planktonic suspension (supernatant) and washing with saline solution 0.85% (v/v), to prevent hydrogel dehydration and to provide fresh medium for the developing biofilm cells, while removing bacteria that were not inside the hydrogel structure. On the other hand, for dual-species biofilm formation, a mixture of both species was prepared using equal volumes of each.

At selected time points (24 and 48h), formation of single and dual-species biofilms was assessed by CFU counts (for cultivable cell counts), DAPI staining (for total cell counts) and LNA/2'OMe-FISH (for total cell counts) as described in the following section. At least two assays were performed for each condition.

3.6 Bacterial Detection within Universal-Bac^{3}Gel

3.6.1 Cultivability Assessment of Biofilms in the Universal-Bac^{3}Gel

At the desired time-points, the number of cultivable biofilm cells was determined by CFU. Briefly, the developed supernatant was removed, and the biofilm formed in the hydrogel was carefully washed with saline solution 0.85% (v/v) to remove loosely attached cells before being dissolved with Bac^{3}Gel dissolution medium [50 mM NaCitrate, pH 7.4]. The volume of dissolution medium used was 1.5× the hydrogel well volume; specifically, 150 µL of dissolution solution was added to each well and let act for about 90 seconds. Afterwards, the remaining solution (dissolved hydrogel plus dispersed biofilm cells) was collected to an Eppendorf and CFU counts were performed. For this purpose, 100 µL of the disrupted biofilm were diluted in 900 µL saline solution 0.85% (v/v) and a series of successive dilutions of 1:10 were conducted. These dilutions were plated in triplicate on TSA for single-species biofilms. For dual-species biofilms, selective media were chosen for easy discrimination of the bacteria, namely, MacConkey agar [Sigma-Aldrich, Germany] and Cetrimide agar [Sigma-Aldrich, Germany] were used to count *K. pneumoniae* and *P. aeruginosa*, respectively. Afterwards, the plates were incubated at 37ºC, overnight. The number of CFU developed were counted and treated as to be expressed in log CFU/mL, as seen in Equation 3.4.

$$\log \frac{CFU}{mL} = \log \left[F \times \frac{CFU_{counts}}{V \times d} \right] \tag{3.4}$$

- CFU_{counts} is the averaged CFU counts;

- F is the dissolution factor and is equal to 2.5;
- V is the volume of the sample used to plate, corresponding to 0.01 mL;
- d is the respective dilution (10^d) in which the CFU were counted.

3.6.2 LNA/2'OMe-FISH and DAPI Staining of Biofilms in the Universal-Bac^{3}Gel

To assess total bacterial cell counts in single- and dual-species biofilms, both FISH protocol and DAPI staining was performed according to Azevedo et. al (2016) [32]. Following biofilm development for 24h and 48h, the existent supernatant was delicately removed from each well exposing the biofilm developed in the hydrogel. The biofilms were then washed with saline solution 0.85% (v/v). Afterwards, the biofilms were fixed and permeabilized during 10 min at room temperature with 100 µL of 4% (v/v) paraformaldehyde and 100 µL of 50% (v/v) ethanol, respectively. After this, the FISH procedure was similar to the one applied for glass slides as described in Section 3.4. Simultaneously, 100 µL hybridization buffer was added to one of the wells to check the autofluorescence of both cells and Universal-Bac^{3}Gel. Given that the hybridization step may cause the biofilm to dry, the wells around the biofilm were filled with distilled water to maintain a humid environment. After hybridization, the probe solution was carefully removed, and the biofilm was immersed in a washing buffer and incubated at 62ºC for 30 min. Once completed, the content of the wells was dissolved with Bac^{3}Gel dissolution medium and pelleted at 15000g for 5 min. The exposed pellet was then resuspended in sterile distilled water and submitted to 6 min of sonication [Elma, Transsonic 420]. This step was carried out so that any aggregates of cells would disrupt, facilitating further cell counting. Afterwards, 20 µL of the sample was placed on a microscope slide and let to dry. On the other hand, a DAPI staining was carried out on the microscope slides with the already dried sample; for that, 20 µL of the DAPI solution was placed over the sample and let act for 10 min. After this time, the sample was thoroughly rinsed with distilled water to remove the excess of DAPI solution. Once more, the sample was placed on an incubator until dried. At this point, the sample is ready to undergo microscopy analysis as described below.

3.7 Microscopy Analysis and Cell Quantification

The samples were imaged using a Nikon ECLIPSE 80i microscope equipped with a Nikon Digital Sight DS-U3 camera and filters capable of detecting the used probes (FITC - EX: 482/35, DM:506, EM:536/40, sensitive to detect Alexa Fluor 488 molecule attached to EUB338 probe, DAPI - EX:387/11, DM:409, EM:447/60, sensitive to detect the DAPI fluorescent stain and SP. Orange - EX:543/22, DM:562, EM: 628/32, sensitive to detect ATTO 550 molecule attached to the species-specific LNA/2'OMe *P. aeruginosa* probe).

The slide was positioned and secured on the microscope's stage and a drop of immersion oil [Nikon, Japan] was placed on top of the sample. The 6× lens was positioned, and necessary adjustments were made using the macro and micrometric knobs for image acquisition. In order to improve image quality, exposure time and gain were adapted to achieve the best signal-to-noise ratio. At least 10 images of representative areas of each sample were used to calculate the total cells/mL.

Cell quantification was carried out with the support of ImageJ software (National Institutes of Health Software, http://rsbweb.nih.gov/ij/index.html).

For coherence, both DAPI and FISH counts were treated to be presented as log cells/mL, as seen in Equation 3.5.

$$\log\frac{cells}{mL} = \log\left[D_{x,t} \times \frac{Counts \times A_{well}}{V_{well} \times A_{image}}\right] \tag{3.5}$$

- $Counts$ corresponds to the averaged LNA/2'OMe-FISH or DAPI counts;

- $D_{x,t}$ is the dilution factor inherent to each biofilm; t corresponds to the biofilm development time and x corresponds to the type of biofilm (single- or dual-species); $D_{P.\ aeruginosa,24h} = D_{K.\ pneumoniae,24h} = D_{dual-species,24h} = 10$; $D_{K.\ pneumoniae,48h} = D_{dual-species,48h} = 7$; $D_{P.\ aeruginosa,48h} = 15$;
- A_{well} is the area of the well of the microscopy slide and is equal to 0.22 cm^2;
- V_{well} is the volume of the well of the microscopy slide and is equal to 0.02 mL;
- A_{image} is the area of the acquired images by microscopy, corresponding to 1.58×10^{-4} cm^2;

3.8 Spatial Organization of Biofilm Populations Using NAM-FISH and CLSM Analysis

To evaluate the feasibility of exploiting LNA/2'OMe-FISH to visualize *in situ* bacterial distribution patterns within the biofilms formed on Universal-Bac^{3}Gel, the FISH protocol was combined with the CLSM analysis. For that, the LNA/2'OMe-FISH procedure was performed, as previously described in Section 3.6.2, for 24h-dual-species biofilms. Afterwards, the intact biofilm was carefully transferred to a 35 mm imaging dish with a polymer coverslip bottom [Ibidi, Germany] to fit the confocal microscope standards. Finally, confocal microscope was used to image the *in situ* hybridized dual-species biofilms, to spatially locate specific bacteria populations within the undisrupted biofilm. For that, a White Light Laser Stellaris 8 (440-790nm) was used for image acquisition. All biofilm samples were scanned using a 63×NA 1.40 oil objective. The following acquisition mode was used: XYZ; image format: 1024 × 1024 pixels; zoom factor of 1; pinhole size: 1 Airy unit; Z-step of 1 µm. The positions within the coupon were randomly selected to avoid bias. Three-dimensional (3D) projections of the biofilms were generated using Imaris Viewer 10.0.1 (https://imaris.oxinst.com/imaris-viewer).

3.9 Statistical Analysis

The obtained data was analyzed by two- or three-way ANOVA with Bonferroni multiple-comparison post-treatment test using GraphPad Prism v.9 for Mac GraphPad Prism Software [San Diego, California USA, www.graphpad.com]. All tests were performed with a confidence level of 95%. For all analysis, *p*-value < 0.05 was considered statistically significant.

4 Results and discussion

Bacterial infections affecting human life quality, specifically associated with CF, have for a long time been associated with polymicrobial biofilms [62]. The continuous improvements in molecular techniques have provided more accurate discrimination of microbial diversity in such infections [123, 124]. It is also known that CF airways are complex environments with oxygen and nutrient gradients [13]; therefore, the use of Universal-Bac^{3}Gel substrates in this study takes microbial culturing one step closer to natural conditions. In this study, single- and dual-species biofilms of the relevant ESKAPE pathogens to CF were quantitatively assessed by culture and molecular techniques. An overview of the conducted experiments is presented in Figure 4.1.

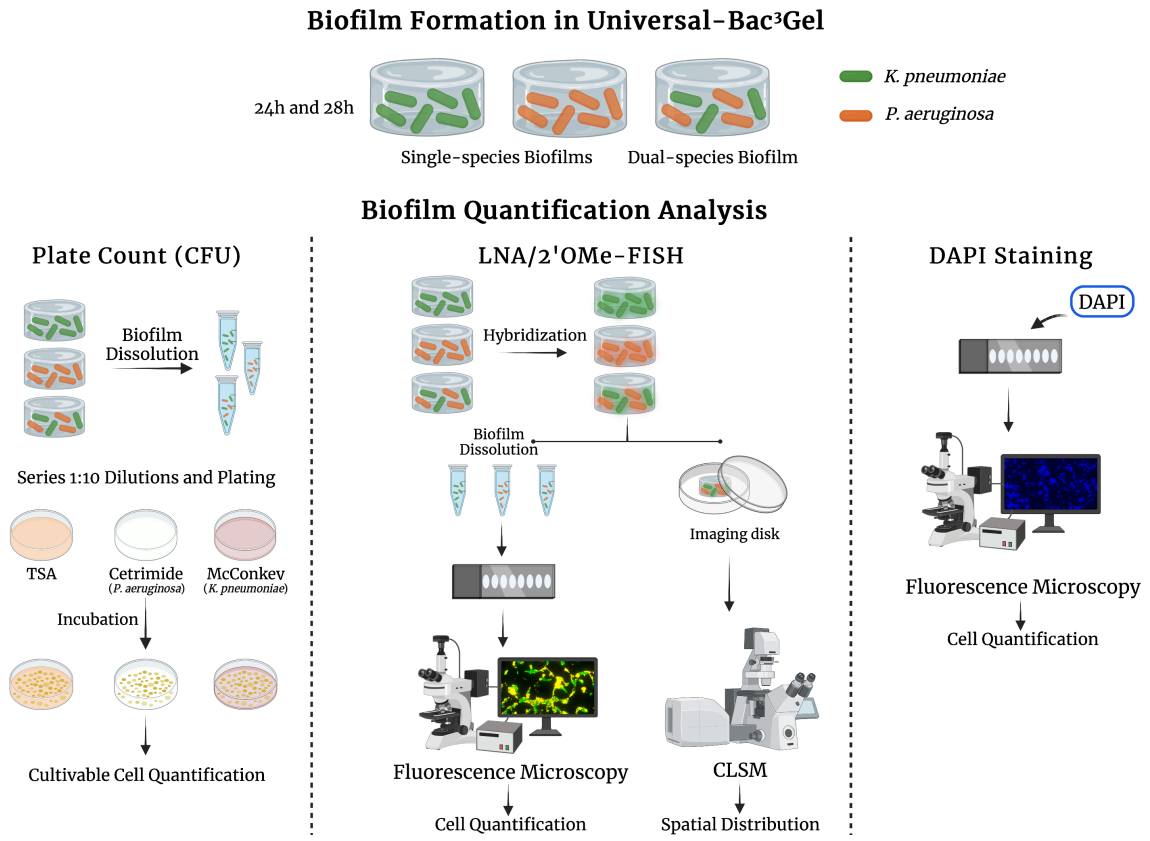

Figure 4.1: Overview of carried out experiments. Single- and dual-species biofilms of *P. aeruginosa* and *K. pneumoniae* were formed in the Universal-Bac^{3}Gel substrate, developing for 24 and 48h. The biofilms were analyzed through CFU, LNA/2'OMe-FISH and DAPI staining. Created with BioRender.com

4.1 Rheological Characterization of Universal-Bac^{3}Gel

Hydrogels can be described as three-dimensional networks that have the ability of retaining large amounts of water in their polymeric structures. They can be formed of biodegradable polymers such as natural polysaccharides (e.g., starch, alginate, agarose) and proteins (e.g., collagen) and thus, have gained interest in the medical field. Their structural and physicochemical properties largely resemble those of EPS produced by bacteria [125, 126]. Rheological characterization of these hydrogels is important to ensure they are fit for their intended purpose and to also optimize final viscoelastic properties. This can be achieved through many tests, namely frequency sweep tests. In this study, it was relevant to determine if the loss and storage moduli are comparable to those of pathological mucus at specific frequencies, corresponding to the normal breathing frequency of 0.5 Hz and ciliary beating of 10Hz [11].

The viscoelastic properties of pathological mucus differ not only between patients, but also with disease progression, type of infection, and even during the day. Indeed, different studies that have performed rheological characterization of CF mucus have reported that G' can vary from 1 to 100 000 Pa, while G''might vary between 0.05 to 100 000 Pa, for the normal and ciliary beating frequencies [11]. The results from the frequency test to the Universal-Bac^{3}Gel substrate are shown in Figure 4.2.

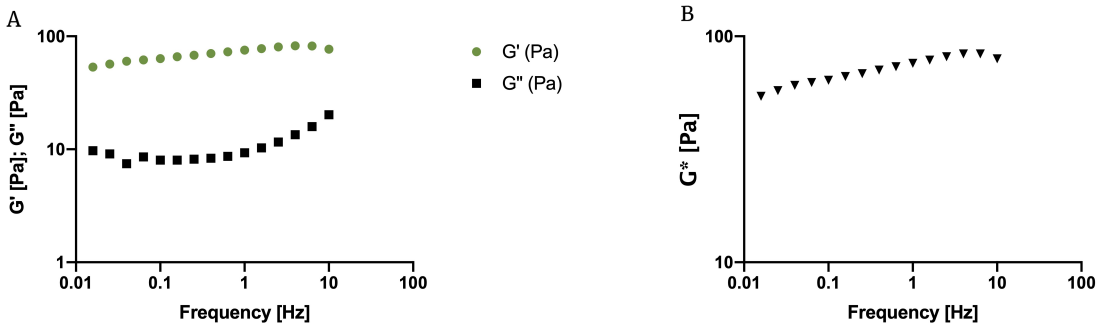

Figure 4.2: Rheological characterization in frequency sweep mode of Universal-Bac^{3}Gel, including G* (Pa), G' (Pa) and G'' (Pa) evaluated from 0.01 to 10 Hz.

Like CF mucus, the viscoelastic properties of Universal-Bac^{3}Gel revealed that G' is higher than G'', which confirms the gel-like behaviour. In terms of magnitude, G'' values ranges from 10 to 30 Pa and G' from 80 to 90 Pa, which are within the range of values reported to CF mucus [11, 82]. Though, as shown in Pedersoli et. al (2021) and Pacheco et. al (2023), these properties can be further customized to reproduce different pathological states [82, 11].

4.2 Performance of LNA/2'OMe-FISH

Preceding the biofilm quantification assays, the performance of the two LNA/2'OMe probes selected for this study was evaluated, according to the optimized conditions reported by Azevedo et. al (2022) [120]. For that, a species-specific *P. aeruginosa* LNA/2'OMe probe attached to ATTO 550 and a universal LNA/2'OMe EUB338 probe attached to Alexa Fluor 488 were used [120]. Ideally, both probes would be species-specific for the selected bacteria for a better discrimination [33]. In fact, both *P. aeruginosa* and *K. pneumoniae* have optimized LNA/2'OMe species-specific probes for multiplex hybridization experiments; although, the fluorescence microscope accessible on our laboratory is equipped with a limited number of filters and the one needed for *K. pneumoniae* species-specific probe visualization was not available. Hence, the LNA/2'OMe EUB338 probe attached to Alexa Fluor 488 (available on the lab) was used to surpass this limitation [120]. Microscopic visualization revealed that both LNA/2'OMe probes showed strong fluorescence at 62ºC, as observed in Figure 4.3.

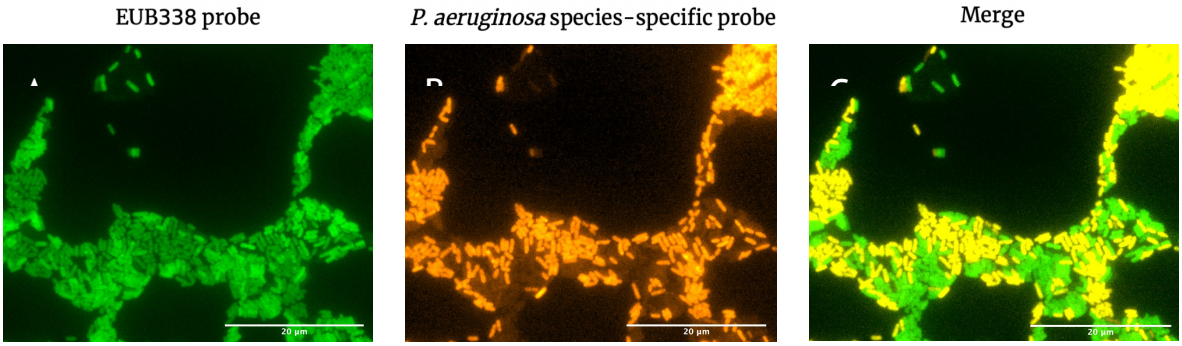

Figure 4.3: Epifluorescence detection of (A) *K. pneumoniae* (green) and (B) *P. aeruginosa* (orange/yellow) using a universal LNA/2'OMe EUB338 probe attached to Alexa Fluor 488 and a species-specific *P. aeruginosa* LNA/2'OMe probe attached to ATTO 550 at 62°C, and (C) both channels merged.

As expected EUB 338 probe hybridized all bacteria [120] (green cells) as shown in Figure 4.3A and it was obtained from observing the sample with FITC filter. Figure 4.3B was obtained by using the Sp. Orange filter and shows only *P. aeruginosa* cells (orange cells). On this figure, it is possible to see a subtle orange shadow, which by merging the two images (Figure 4.3C), it was possible to conclude that it corresponds to *K. pneumoniae* cells. This combination of LNA/2'OMe probes allowed for a sufficient discrimination of both bacteria.

4.3 LNA/2'OMe-FISH Method Development and Validation in Universal-Bac^{3}Gel

After testing the multiplex assay on smears, the following goal was to apply and validate the LNA/2'OMe-FISH protocol on biofilms cultured in the Universal-Bac^{3}Gel substrate. To this purpose, the LNA/2'OMe-FISH protocol was performed on a single-species biofilm of *P. aeruginosa*. Upon microscopy visualization, the hybridization appeared to be successful; although, the acquired images revealed many bacterial aggregates (Figure A.1A, Appendix A), which was not desired since it would hinder further cell quantification. Two different approaches were tested for cell dispersion. The first possibility involved a pre-microscopy treatment of the cells with Tween 80 and EDTA, though it revealed to increase the aggregation of cells (Figure A.1B, Appendix A), so it was promptly discarded. The other possibility consisted on submitting the sample to an ultrasound bath during different times. Different periods of time were tested and the minimum amount of time to avoid cell clusters was found to be 6 min (Figure A.1C, Appendix A).

Afterwards, the feasibility of exploiting the LNA/2'OMe-FISH technique for quantification of biofilm cells grown within the Universal-Bac^{3}Gel was tested. To this, a comparison of cell counts by LNA/2'OMe-FISH at both 24 and 48h and DAPI counts for the *P. aeruginosa* single-species biofilms was performed (Figure 4.4). The results showed that the percentage of cells detected by LNA/2'OMe-FISH in comparison with DAPI was around 84% (Figure 4.4A), for both 24 and 48h (p>0.05). Almeida et. al (2011) performed a similar analysis, however with a different type of NAM (PNA) and achieved PNA-FISH counts equal to more than 90% of DAPI counts [33]. This difference might be explained by the NAMs nature. NAM characteristics, such as size and charge, are decisive to the success of hybridization since probes must endure a path through the biofilm matrix and cell wall. Typically, both LNA/2'OMe and PNA probes present roughly the same size (~15 bp); however, their charge varies. In fact, PNA probes contain no charged phosphate groups, which means they suffer less electrostatic repulsion [7], providing for an effortless biofilm and cell penetration. On the other hand, LNA/2'OMe probes hold a negative charge [6], therefore there might be more resistance in their path to hybridization. This characteristic is one of the reasons for the notoriety of PNA probes amongst FISH techniques in biofilm research. Regardless, LNA/2'OMe are still appointed as promising probes for biofilm studies due to their enhanced hybridization efficiency with nucleic acids (in comparison to PNA), high water solubility and design flexibility [7, 118].

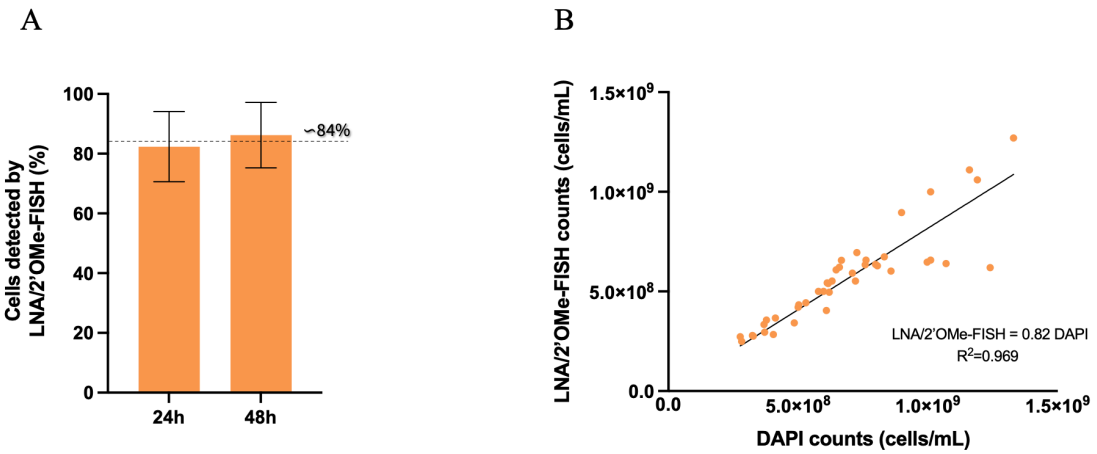

Figure 4.4: Validation of LNA/2'OMe-FISH method. (A) Percentage of cells detected by LNA/2'OMe-FISH for 24 and 48h *P. aeruginosa* biofilms (data shown is the average percentage of the quotient of cells detected by LNA/2'OMe-FISH and DAPI; error bars are the standard deviation (SD)); (B) Correlation between FISH and

DAPI counts (cells/mL) for *P. aeruginosa* single-species biofilm (each point represents the cell counts of LNA/2'OMe-FISH and DAPI; line represents the adjustment of the points to a linear regression model (slope=0.817 and $R^2 = 0.969$).

For additional validation of the method, a correlation between LNA/2'OMe-FISH and DAPI counts for 24 and 48h of the single-species biofilm of *P. aeruginosa* was performed, as shown in Figure 4.4B. These values are well adjusted ($R^2 = 0.969$) to a linear regression with slope equal to 0.817, which means that LNA/2'OMe-FISH detects around 82% of DAPI counts, corroborating the results from Figure 4.4A. The same behavior was also observed by Almeida et. al (2011) [33]. These results prove that LNA/2'OMe-FISH is a reliable technique for detection and discrimination of bacterial cells within a biofilm and can be implemented on biofilms cultured in advanced 3D substrates, such as the Universal-Bac^{3}Gel.

4.4 Single- and Dual-Species Biofilms Cultured in Universal-Bac^{3}Gel

Taking advantage of the previously validated LNA/2'OMe method, the next goal was to evaluate the bacteria's ability to form single- and dual-species biofilms within the Universal-Bac^{3}Gel substrate. For that purpose, *P. aeruginosa* and *K. pneumoniae* were mono- and co-cultured in that substrate, and after 24 and 48h of development, cell counts were assessed by CFU, LNA/2'OMe-FISH and DAPI. This analysis will allow to determine the behaviour and dynamics of the biofilm species within the 3D structure. Total biofilm counts for single- and dual-species biofilms by the different analytical methods are presented in Figure 4.5.

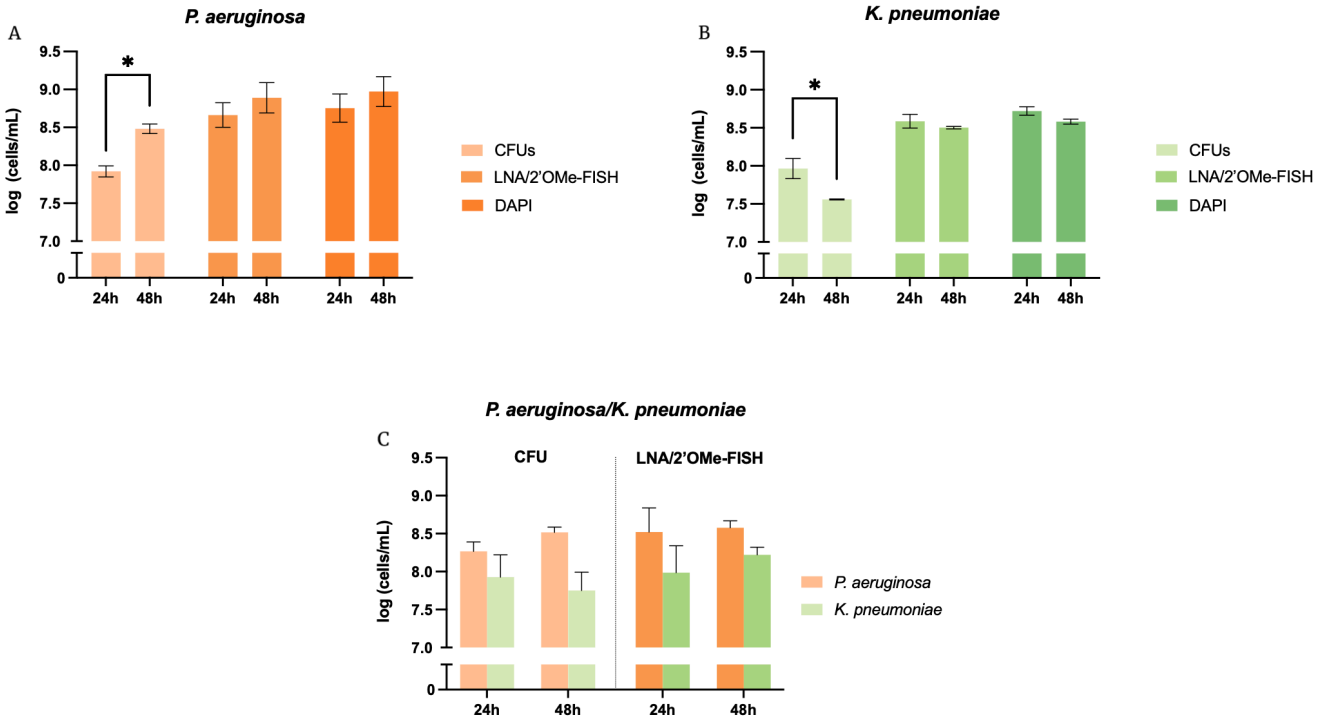

Figure 4.5: Biofilm quantification by CFU, LNA/2'OMe-FISH and DAPI. (A) Total counts estimated for single-species biofilms of *P. aeruginosa* expressed as log cells/mL; (B) Total counts estimated for single-species biofilms of *K. pneumoniae* expressed as log cells/mL; (C) Total counts estimated for dual-species biofilms of *P. aeruginosa* and *K. pneumoniae* expressed as log cells/mL) * Statistically significant: $p < 0.05$ (Data shown are average; n 2; error bars indicate SD).

Concerning the single-species biofilms culturability for 24 and 48h, the CFU counts of both species significantly varied ($p<0.05$), presenting values ranging from log 7.6 and log 7.9 cells/mL (for *K. pneumoniae*, 48 and 24h, respectively) to log 7.9 and log 8.5 cells/mL (for *P. aeruginosa*, 24 and 48h, respectively). As expected, the number of *P. aeruginosa* biofilm culturable cells increased with time of culture (Figure 4.5A) [127]. Additionally, LNA/2'OMe-FISH and DAPI counts have also increased from log 8.7 to log 8.9 cells/mL and log 8.8 to log 9 cells/mL, respectively, but neither growth was significant ($p>0.05$). As for *K. pneumoniae*, the opposite behaviour was observed since all methods revealed less

biofilm cells at 48h than at 24h (log 8.6 to log 8.5 cells/mL and log 8.7 to log 8.6 cells/mL, for LNA/2'OMe-FISH and DAPI, respectively; Figure 4.5B). Although not significant (p>0.05), this behaviour was not expected in this study since no stress factors (e.g., antibiotics) were introduced and is also not consistent with previous *K. pneumoniae* biofilm tests. In a previous experiment, the ability of *K. pneumoniae* to form biofilms was assessed through its cultivation on microtiter plates and subsequent CV staining and biomass quantification analysis, revealing increased biofilm formation ability that peaked at 5 days (120h) and only then started to decline [128, 129]. This unexpected result might be due to some experimental error and for this reason more repetitions are needed to understand if this behaviour persists.

For both species, it was observed that CFU counts are always significantly lower than LNA/2'OMe-FISH and DAPI counts (p<0.05), which was expected [33]. In fact, in the CFU method, only culturable bacteria are being counted since dead bacteria can no longer grow nor divide in culture media [130]. Another reason contributing to this disparity lies in the concept of viable but non-culturable bacteria (VBNC). During biofilm formation, environment stresses (e.g., nutrient scarcity, water limitation, extreme concentrations, temperatures and pH) may induce cells to enter a starvation survival state, in which cells are not dead but can no longer be cultured [83]. Contrarily, LNA/2'OMe probes and DAPI hybridize all cells present, despite their viability, which simply means that all cells, death or alive, will be hybridized and therefore counted [131, 6].

In dual-species biofilms, the number of culturable cells of *P. aeruginosa* slightly increased from log 8.3 to log 8.5 CFU/mL from 24 to 48h, respectively. As for *K. pneumoniae*, at 24h cultivability was log 8 CFU/mL and for 48h decreased 0.2 log CFU/mL (Figure 4.5C). Although, both variations were statistically insignificant (p>0.05), in comparison to each species cultivability in single-species biofilms, it is possible to claim that generally, the number of viable cells present at each time was similar. Additionally, in co-culture, *P. aeruginosa* revealed similar values of LNA/2'OMe-FISH counts for the considered times (log 8.6 cells/mL). For *K. pneumoniae* in mixed biofilm, these values presented a slight increase from log 8 to log 8.2 cells/mL (p>0.05). Overall, for dual-species biofilms, *P. aeruginosa* cultivability and LNA/2'OMe-FISH cell counts were higher than *K. pneumoniae*. This observation agrees with a previous study, that aimed to assess the biofilm formation ability of different *K. pneumoniae* mutants in co-culture with *P. aeruginosa* and revealed that *P. aeruginosa* represents a bigger share of the biofilm biomass compared to *K. pneumoniae* [132, 133].

P. aeruginosa dual-species biofilm cell counts (either CFU or LNA/2'OMe-FISH) were similar to single-species counts, which was expected. Actually, studies have shown that when cultured with other bacteria, for times between 24 and 48h, *P. aeruginosa* does not show significant differences in growth [134, 129]. Additionally, *K. pneumoniae* revealed a slight decrease in LNA/2'OMe-FISH counts from single- to dual-species biofilm (p>0.05). This means that *K. pneumoniae*'s ability to form biofilms was barely affected by the presence of *P. aeruginosa*, which has also been previously observed [135]. This behaviour is not always verified since *P. aeruginosa* is commonly reported as an antagonistic microorganism, in both planktonic and sessile culture [132]; in fact, this species has been reported to kill or hinder growth of other CF infections-related microorganism, such as *Candida albicans* [136, 133] and *S. aureus* [137, 133]. The observed behaviour in this work was not expected since, in 2022, a study aiming to test the anti-biofilm capacity of bacterial supernatants revealed that *K. pneumoniae* showed reduced biofilm formation when cultured in the presence of the supernatant from an overnight growth of *P. aeruginosa* [138]. Additionally, a study by Zhao et. al (2018) has revealed that when in co-culture, *P. aeruginosa* significantly suppresses the growth of *K. pneumoniae*, comparatively to mono-culture. The same study has revealed that *P. aeruginosa* was predominant when in co-culture with *K. pneumoniae* and reported that both species are capable of forming stable *in vitro* biofilms, corroborating the results from this work [139].

In summary, both species revealed the ability to form single- and dual-species biofilms in the Universal-Bac^{3}Gel substrate, achieving cell counts as high as in other *in vitro* models.

4.5 Spatial Organization of Biofilms Cultured in Universal-Bac^{3}Gel by LNA/2'OMe-FISH

The spatial distribution of the diverse bacteria within a polymicrobial biofilm can provide valuable information on the species interactions. Diverse species in polymicrobial biofilms can be organized essentially in three ways, i.e., separate mono-species microcolonies, co-aggregation and in layers (as described in Section 2.1, Figure 2.1) [30]. To elucidate on *P. aeruginosa* and *K. pneumoniae* 3D architecture and infer about their interactions, the LNA/2'OMe technique was combined with CLSM to analyze a 24h-dual-species biofilm (Figure 4.6). It is relevant to mention that the Universal-Bac^{3}Gel substrate has about 2 mm of height and the confocal microscope only allowed for the visualization of a part of the hydrogel, therefore the acquired images do not correspond to the whole biofilm, but only to the bottom 60 µm.

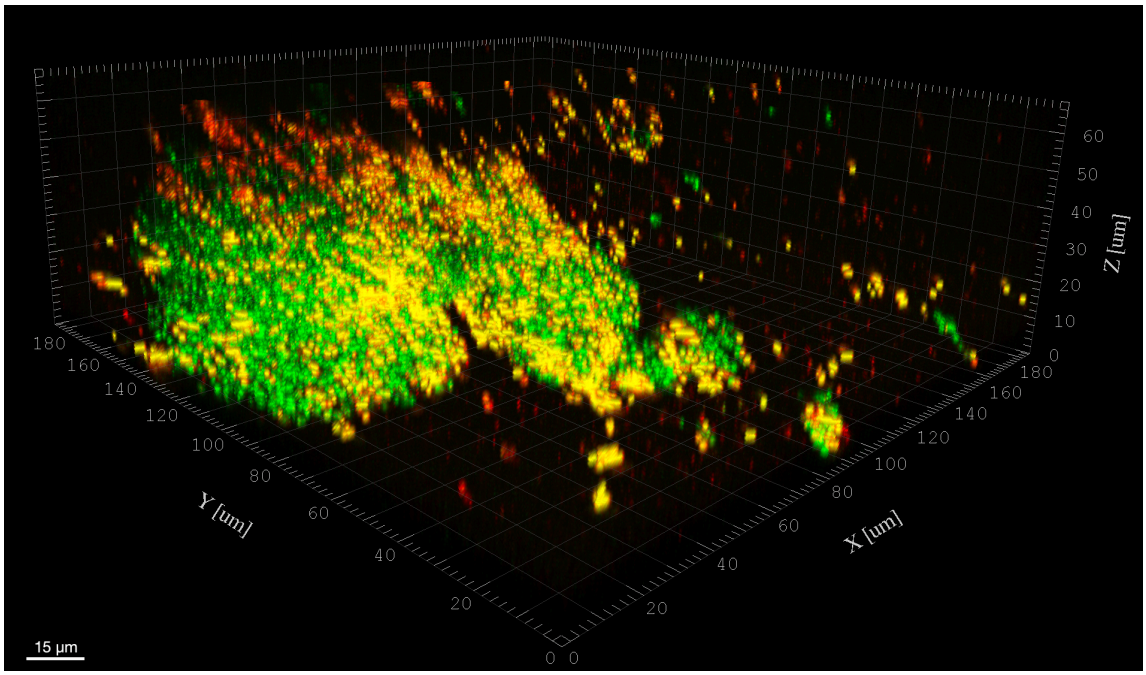

Figure 4.6: CLSM 3D image of 24h-dual-species biofilms of *P. aeruginosa* (orange/yellow cells) and *K. pneumoniae* (green cells) grown in Universal-Bac^{3}Gel.

Visual inspection of this fraction of the biofilm, suggests a higher abundance of green bacteria (*K. pneumoniae*) compared to orange/yellow bacteria (*P. aeruginosa*), contrary to what would be expected from the previous quantification results. Actually, it is possible that *P. aeruginosa* is not so abundant in the bottom part of the biofilm and the majority of its cells are located on the upper part of the biofilm. Since *P. aeruginosa* generally outnumbered *K. pneumoniae*, it is reasonable to state that the first might preferably colonize the region with most oxygen access. In fact, being a facultative anaerobe, *P. aeruginosa* can adapt to low/no oxygen environments but prefers to grow under aerobic conditions [140, 141]. This observation is supported by a report from Lopes et. al (2018), that quantitatively evaluated (through PNA-FISH) the biofilm formation ability of a consortia of the prominent CF pathogen, *P. aeruginosa*, and other two atypical pathogens, through different oxygen concentrations (aerobic, microaerophilic and anaerobic). This study revealed that *P. aeruginosa* in dual- and triple-species biofilms exhibited a tendency to decrease cell counts by PNA-FISH with the decrease of oxygen availability, demonstrating that *P. aeruginosa* in co-culture preferably grows in aerobic environment [13].

Regarding the three possible organizations mentioned above, it is possible to observe that the two species in this biofilm exhibit a co-aggregation arrangement. To clearly demonstrate it, 4 equidistant (10 µm apart) z plane section images were captured and displayed on a 3D axis (Figure 4.7).

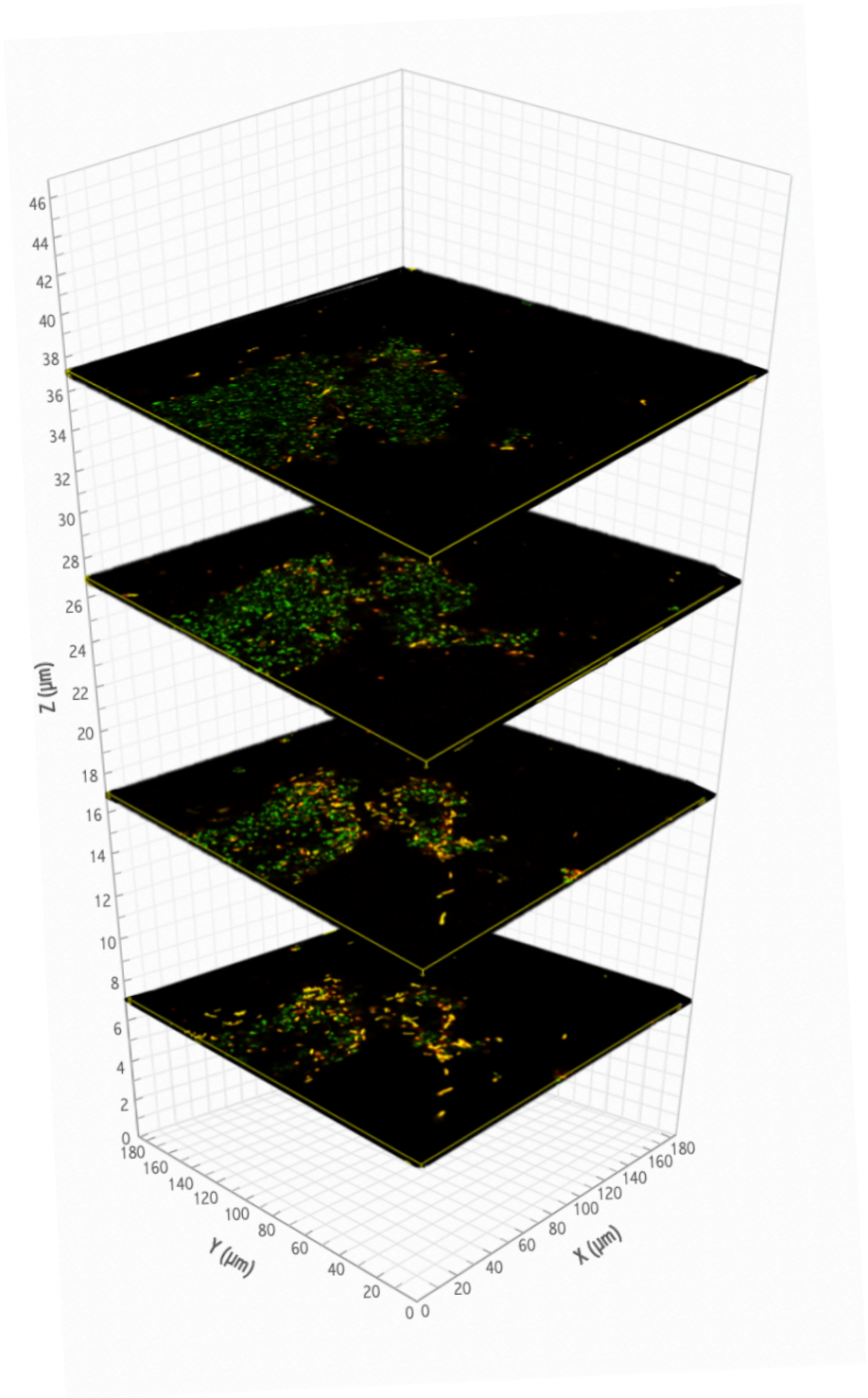

Figure 4.7: Display of 4 equidistant z plane section images of the Universal-Bac^{3}Gel cultured biofilm on a 3D axis. Planes represented correspond to z=7, 17, 27 and 37 µm. Green cells represent *K. pneumoniae*; orange/yellow cells represent *P. aeruginosa*.

In each plane it is possible to observe individual *P. aeruginosa* and *K. pneumoniae* cells mixed together, therefore corroborating the co-aggregation organization. This type of distribution is characteristic of cooperative or synergistic interactions between the species [30, 142], which indicates that, for this study, the association of the two microbes may be neutral or even beneficial. This kind of interaction was expected since no drastically reduction on cell counts were observed for any species regarding the dual-species biofilm. The fact that *P. aeruginosa* still outnumbered *K. pneumoniae* regarding cell production in co-culture does not implicate that an antagonistic relation was established, since the abundance of a species does not necessarily relate to its role in the consortium [129]. Indeed, a similar observation was made by

Azevedo et. al (2016) when studying the biofilm forming ability and spatial distribution of dual-species biofilms of *E. coli* with *Delftia tsuruhatensis* and *E. coli* with *Achromobacter xylooxidans*. In this assay, E. coli outnumbered both species in their respective biofilm, but upon CLSM analysis, the bacteria appeared to be mixed, revealing a synergistic/neutral relation [32].

Additionally, *P. aeruginosa* has shown the same type of spatial distribution (co-aggregation) with other microbes in dual-species biofilms. Cerqueira et. al (2013) combined PNA-FISH with CLSM to visualize the spatial organization of dual-species biofilm of *E. coli* and *P. aeruginosa* and also observed a co-aggregated distribution [143].

LNA/2'OMe-FISH allied with CLSM has proved to be a reliable technique for discrimination of species and visualization of their spatial distribution within biofilms without destroying its 3D structure.

5 Conclusion and Future Perspectives

5.1 Conclusion

Biofilms have impact on various fields, whether beneficial or detrimental. Particularly in health, biofilms hold great protagonism since they are the source of most infections [8]. Various bacterial infections have been studied and revealed that most of them are polymicrobial, i.e., most infections are caused by biofilms formed not from one but from a consortium of microorganisms. These infections are accountable for a great share of hospitalized patients' mortality. Therefore, the impact of biofilms in health cannot be ignored and more efforts should be put into their understanding, whether it is to prevent or simply control them [38, 39]. Regarding biofilm research, it is of the utmost importance that natural environment conditions are closely recreated in the labs for producing the most reliable results.

This work aimed at expanding our knowledge on biofilms by adopting two innovative technologies to both culture and analyze biofilm formation and dynamics; specifically, this worked sought the implementation and validation of LNA/2'OMe-FISH on biofilms composed of relevant pathogens to CF (*P. aeruginosa* and *K. pneumoniae*), cultured in Universal-Bac^{3}Gel substrate, which seeks to mimic general properties of the human mucus. Additionally, it was intended to combine this technique with CLSM to draw conclusions about the spatial distribution of these microorganisms in the biofilm and to infer about the type of interaction they develop in dual-species biofilms.

Firstly, by the rheological characterization of the Universal-Bac^{3}Gel, it was concluded that this advanced substrate presents characteristics that are generally comparable to the CF mucus airways; although, these can be further customized to replicate different pathological states [82, 11].

After ensuring LNA/2'OMe-FISH probes performance, the method was implemented in single-species biofilm of *P. aeruginosa* and validated by comparison with another biofilm analysis method, DAPI staining. The validation results revealed that LNA/2'OMe-FISH is capable of detecting around 84% of the cells detected by DAPI, with counts from both methods presenting a correlation coefficient of 0.969. These results allowed validation of the LNA/2'OMe-FISH as a reliable and robust technique for identification, discrimination and cell quantification of biofilms cultured in Universal-Bac^{3}Gel.

Once the reliability of this method was proven, it was applied for the analysis of single- and dual-species biofilms of *P. aeruginosa* and *K. pneumoniae*, cultured for 24 and 48h. At this stage, CFU analysis was also conducted to provide information on the number of total cultivable cells in the biofilm. The development of biofilms over time for each species revealed that *P. aeruginosa* biofilm cell counts increased with biofilm development time, unlike *K. pneumoniae*, which presented higher biofilm cell counts at 24h. As discussed in Section 4.4, the first result is in line with what was expected and reported in the literature, but the second is not. No literature support was found for this behaviour. For dual-species biofilms, it was observed that these species were able to form biofilm and reach values of total cells (detected by LNA/2'OMe-FISH) similar to those achieved in single-species, which suggests that these species have cooperative/neutral interactions rather than antagonistic, since none of them experienced a significant reduction in total cell counts in dual- compared to single-species biofilm. Regarding the number of CFUs, it was observed that for single- and dual-species biofilms, the number of viable cells was always lower than those detected by LNA/2'OMe-FISH or DAPI, as expected. With these results, it was possible to conclude that both species have the ability form single- and dual-species biofilms in Universal-Bac^{3}Gel substrate.

Finally, through the combination of LNA/2'OMe-FISH with CLSM, it was possible to conclude that the species were mixed in the volume of the analyzed biofilm sample and therefore are co-aggregated. This configuration is characteristic of biofilms in which species cooperate, or at least do not harm each other.

Overall, it is possible to conclude that LNA/2'OMe-FISH can be successfully implemented to analyze single- or dual-species biofilms cultured in Universal-Bac^{3}Gel and allows for characterization of the spatial distribution of species within the biofilm.

5.2 Future Perspectives

Several tests can be carried out to consolidate and add information to the present conclusions. Concerning the new 3D substrate used for biofilm culture and its properties, it would be interesting to perform a rheological test to the substrate after biofilm formation, to see how the biofilm affects the properties of the hydrogel, namely its viscoelasticity. Still regarding the formation of biofilms, it would be important to culture these same bacteria in the specific customized substrate of CF produced by Bac^{3}Gel. This substrate is bioinspired in cystic fibrosis mucus, so it replicates even more accurately most features of the CF airways, such as composition, gradient structure and viscoelastic properties [82]. In a step forward, the chemical composition (i.e., presence of mucin in Cystic Fibrosis-Mu^{3}Gel (CF-Mu^{3}Gel) could be considered to determine how mucin impacts biofilm growth, behaviour and organization. Along these lines, it would also be relevant to culture in this substrate other bacteria commonly found in CF lung infections (over 100 different genus, and consequently much more species, of microbes have been isolated from the respiratory tract of CF patients so far [53, 2] and perform LNA/2'OMe-FISH multiplex assays.

Additionally, it would be valuable to perform pre-colonization assays with the relevant pathogens of CF. *S. aureus* infections in CF airways are reported to happen at a very early stage, prior to other pathogens colonization, specifically *P. aeruginosa* [64]; hence, it would be pertinent to recreate this timeline and inoculate the CF-Mu^{3}Gel with *S. aureus* followed by *P. aeruginosa*. Since this work focuses on biofilms that directly affect human health and MDR microbes are an urgent issue, it should also be considered to perform a biofilm susceptibility assay with clinically relevant antibiotics, particularly to CF, such as tobramycin and gentamicin.

Regarding microscopy, in this work only a fraction of the biofilm was possible to be observed by CLSM. In this sense, it would be interesting to make cuts in the substrate with the formed biofilm before microscopy analysis. This would allow visualizing of the spatial distribution of the species in each fraction of the biofilm and thus it would be possible to make a 3D reconstruction of the biofilm. Alternatively, the LNA/2'OMe-FISH technique could also be implemented for biofilm visualization with multiphoton laser scanning microscopy (MLSM), which presents many advantages over CLSM, such as deeper imaging depth [144].

Finally, it would be interesting to implement LNA/2'OMe-FISH to real biofilm samples (from CF airways mucus) and visualize them under CLSM/MLSM to assess if the spatial distribution compares to the one observed of biofilms cultured in CF-Mu^{3}Gel.

6 References

[1] C. Michaelis and E. Grohmann, "Horizontal gene transfer of antibiotic resistance genes in biofilms," *Antibiotics*, vol. 12, no. 2, p. 328, 2023.

[2] S. P. Lopes, N. F. Azevedo, and M. O. Pereira, "Microbiome in cystic fibrosis: shaping polymicrobial interactions for advances in antibiotic therapy" *Critical reviews in microbiology*, vol. 41, no. 3, pp. 353-365, 2015.

[3] A.Barbosa, S.Miranda, N.F.Azevedo, L.Cerqueira, and A.S.Azevedo, "Imaging biofilms using fluorescence *in situ* hybridization: seeing is believing," *Frontiers in Cellular and Infection Microbiology*, vol. 13, p. 1195803, 2023.

[4] I. Guzman-Soto, C. McTiernan, M. Gonzalez-Gomez, A. Ross, K. Gupta, E. J. Suuronen, T. F. Mah, M. Griffith, and E. I. Alarcon, "Mimicking biofilm formation and development: Recent progress in in vitro and *in vivo* biofilm models," *Iscience*, vol. 24, no. 5, 2021.

[5] K. Sauer, P. Stoodley, D. M. Goeres, L. Hall-Stoodley, M. Burmølle, P. S. Stewart, and T. Bjarnsholt, "The biofilm life cycle: Expanding the conceptual model of biofilm formation," *Nature Reviews Microbiology*, vol. 20, no. 10, pp. 608–620, 2022.

[6] R. Oliveira, A. S. Azevedo, and L. Mendes, "Application of nucleic acid mimics in fluorescence *in situ* hybridization," *Fluorescence In-Situ Hybridization (FISH) for Microbial Cells: Methods and Concepts*, pp. 69–86, 2021.

[7] M. Nácher-Vázquez, B. Santos, N. F. Azevedo, and L. Cerqueira, "The role of nucleic acid mimics (nams) on fish-based techniques and applications for microbial detection," *Microbiological Research*, vol. 262, p. 127086, 2022.

[8] S. K. Yadav and S. Sanyal, "Biofilms: The good and the bad," *Biofilms in Human Diseases: Treatment and Control*, pp. 13–26, 2019.

[9] S.Srivastava and A.Bhargava, "Biofilms and human health" *Biotechnology letters*, vol.38, pp. 1–22, 2016.

[10] R. M. Donlan and J. W. Costerton, "Biofilms: survival mechanisms of clinically relevant microorganisms," *Clinical microbiology reviews*, vol. 15, no. 2, pp. 167–193, 2002.

[11] D. Pacheco, F. Bertoglio, C. Butnarasu, N. S. Vargas, G. Guagliano, A. Ziccarelli, F. Briatico-Vangosa, V. Ruzzi, S. Buzzaccaro, R. Piazza et al., "Heterogeneity governs 3D-cultures of clinically relevant microbial communities," 2023.

[12] J. Azeredo, N. F. Azevedo, R. Briandet, N. Cerca, T. Coenye, A. R. Costa, M. Desvaux, G. Di Bonaventura, M. Hébraud, Z. Jaglic et al., "Critical review on biofilm methods," *Critical reviews in microbiology*, vol. 43, no. 3, pp. 313–351, 2017.

[13] S. P. Lopes, N. F. Azevedo, and M. O. Pereira, "Quantitative assessment of individual populations within polymicrobial biofilms," *Scientific reports*, vol. 8, no. 1, p. 9494, 2018.

[14] G.Batani, K.Bayer, J.Böge, U.Hentschel, and T.Thomas, "Fluorescence *in situ* hybridization (FISH) and cell sorting of living bacteria," *Scientific reports*, vol. 9, no. 1, p. 18618, 2019.

[15] N. M. Guimarães, N. F. Azevedo, and C. Almeida, "Fish variants," *Fluorescence In Situ Hybridization (FISH) for Microbial Cells: Methods and Concepts*, pp. 17–33, 2021.

[16] L. Cerqueira, N. F. Azevedo, C. Almeida, T. Jardim, C. W. Keevil, and M. J. Vieira, "DNA mimics for the rapid identification of microorganisms by fluorescence *in situ* hybridization (FISH)," *International Journal of Molecular Sciences*, vol. 9, no. 10, pp. 1944–1960, 2008.

[17] R. C. van de Vijsel, J. van Belzen, T. J. Bouma, D. van der Wal, V. Cusseddu, S. J. Purkis, M. Rietkerk, and J. van de Koppel, "Estuarine biofilm patterns: modern analogues for pre-cambrian self-organization," *Earth Surface Processes and Landforms*, vol. 45, no. 5, pp. 1141–1154, 2020.

[18] R. Chandki, P. Banthia, and R. Banthia, "Biofilms: A microbial home," *Journal of Indian Society of Periodontology*, vol. 15, no. 2, p. 111, 2011.

[19] H. C. Flemming, J. Wingender, U. Szewzyk, P. Steinberg, S. A. Rice, and S. Kjelleberg, "Biofilms: an emergent form of bacterial life," *Nature Reviews Microbiology*, vol. 14, no. 9, pp. 563–575, 2016.

[20] S. Kumar, A. Srivastava, and S. Rastogi, "An introduction to microbial biofilm," *Biofilms in Human Diseases: Treatment and Control*, pp. 1–12, 2019.

[21] N. Høiby, "A short history of microbial biofilms and biofilm infections," *Apmis*, vol. 125, no. 4, pp. 272–275, 2017.

[22] J. Allkja and A. S. Azevedo, "Characterization of social interactions and spatial arrangement of individual bacteria in multistrain or multispecies biofilm systems using nucleic acid mimics-fluorescence *in situ* hybridization," *Fluorescence In-Situ Hybridization (FISH) for Microbial Cells: Methods and Concepts*, pp. 97–109, 2021.

[23] C. F. Rodrigues, J. Allkja, L. Mendes, and A. S. Azevedo, "Methods for the visualization of multispecies biofilms," in *Multispecies Biofilms: Technologically Advanced Methods to Study Microbial Communities. Springer*, 2022, pp. 35–78.

[24] A. Orell, S. Schopf, L. Randau, and M. Vera, "Biofilm lifestyle of thermophile and acidophile archaea," *Biocommunication of Archaea*, pp. 133–146, 2017.

[25] S. Fanning and A. P. Mitchell, "Fungal biofilms," *PLoS pathogens*, vol. 8, no. 4, p. e1002585, 2012.

[26] Y. T. Cheah and D. J. C. Chan, "Physiology of microalgal biofilm: a review on prediction of adhesion on substrates," *Bioengineered*, vol. 12, no. 1, pp. 7577–7599, 2021.

[27] L. Nistico, L. Hall-Stoodley, and P. Stoodley, "Imaging bacteria and biofilms on hardware and periprosthetic tissue in orthopedic infections," *Microbial Biofilms: Methods and Protocols*, pp. 105–126, 2014.

[28] Z. Khatoon, C. D. McTiernan, E. J. Suuronen, T.-F. Mah, and E. I. Alarcon, "Bacterial biofilm formation on implantable devices and approaches to its treatment and prevention," *Heliyon*, vol. 4, no. 12, 2018.

[29] Y. Chao and T. Zhang, "Surface-enhanced raman scattering (sers) revealing chemical variation during biofilm formation: from initial attachment to mature biofilm," *Analytical and bioanalytical chemistry*, vol. 404, pp. 1465–1475, 2012.

[30] S. Elias and E. Banin, "Multi-species biofilms: living with friendly neighbors," *FEMS microbiology reviews*, vol. 36, no. 5, pp. 990–1004, 2012.

[31] C. Y.Chang, "Surface sensing for biofilm formation in *Pseudomonas aeruginosa*" *Frontiers in microbiology*, vol. 8, p. 2671, 2018.

[32] A. S. Azevedo, C. Almeida, B. Pereira, L. F. Melo, and N. F. Azevedo, "Impact of delftia tsuruhatensis and achromobacter xylosoxidans on Escherichia coli dual-species biofilms treated with antibiotic agents," *Biofouling*, vol. 32, no. 3, pp. 227–241, 2016.

[33] C. Almeida, N. F. Azevedo, S. Santos, C. W. Keevil, and M. J. Vieira, "Discriminating multi-species populations in biofilms with Peptide Nucleic Acid-Fluorescence *in situ* Hybridization (PNA-FISH)," *PloS one*, vol. 6, no. 3, p. e14786, 2011.

[34] S. Veerachamy, T. Yarlagadda, G. Manivasagam, and P. K. Yarlagadda, "Bacterial adherence and biofilm formation on medical implants: a review," *Proceedings of the Institution of Mechanical Engineers, Part H: Journal of Engineering in Medicine*, vol. 228, no. 10, pp. 1083–1099, 2014.

[35] V. Preda and O. Sandulescu, "Communication is the key: biofilms, quorum sensing, formation and prevention," *Discoveries*, vol. 7, p. e10, 09 2019.

[36] R.Funari and A.Q.Shen, "Detection and characterization of bacterial biofilms and biofilm-based sensors," *ACS sensors*, vol. 7, no. 2, pp. 347–357, 2022.

[37] M. Crouzet, C. Le Senechal, V. S. Brözel, P. Costaglioli, C. Barthe, M. Bonneu, B. Garbay, and S. Vilain, "Exploring early steps in biofilm formation: set-up of an experimental system for molecular studies," *BMC microbiology*, vol. 14, no. 1, pp. 1–12, 2014.

[38] M. Sen and P. Yadav, "Modern methods in microscopy for the assessment of biofilms," *Biofilms in Human Diseases: Treatment and Control*, pp. 59–69, 2019.

[39] S.Dubey, S.Dubey, A.Gupta and V.Sharma, "Biofilm-mediated dental diseases", *Biofilms in Human Diseases: Treatment and Control*, pp. 91–116, 2019.

[40] S. Santajit, N. Indrawattana et al., "Mechanisms of antimicrobial resistance in eskape pathogens," *BioMed research international*, vol. 2016, 2016.

[41] A. Monteiro, J. Cardoso, N. Guerra, E. Ribeiro, C. Viegas, S. Cabo Verde, and A. Sousa-Uva, "Exposure and health effects of bacteria in healthcare units: An overview," *Applied Sciences*, vol. 12, no. 4, p. 1958, 2022.

[42] C. J. Kristich, L. B. Rice, and C. A. Arias, "Enterococcal infection treatment and antibiotic resistance," *Enterococci: from commensals to leading causes of drug resistant infection*, 2014.

[43] M. Qodrati, S. SeyedAlinaghi, S. A. DehghanManshadi, A. Abdollahi and O. Dadras, "Antimicrobial susceptibility testing of staphylococcus aureus isolates from patients at a tertiary hospital in Tehran, Iran, 2018–2019," *European Journal of Medical Research*, vol. 27, no. 1, p. 152, 2022.

[44] Y. Li, S. Kumar, L. Zhang, and H. Wu, "*Klebsiella pneumonia*e and its antibiotic resistance: a bibliometric analysis," *BioMed Research International*, vol. 2022, 2022.

[45] M. Wu and X. Li, "*Klebsiella pneumoniae* and *Pseudomonas aeruginosa*," in *Molecular medical microbiology*. Elsevier, 2015, pp. 1547–1564.

[46] I. Kyriakidis, E. Vasileiou, Z. D. Pana, and A. Tragiannidis, "*Acinetobacter baumannii* antibiotic resistance mechanisms," *Pathogens*, vol. 10, no. 3, p. 373, 2021.

[47] Z. Pang, R. Raudonis, B. R. Glick, T.-J. Lin, and Z. Cheng, "Antibiotic resistance in *Pseudomonas aeruginosa*: mechanisms and alternative therapeutic strategies," *Biotechnology advances*, vol. 37, no. 1, pp. 177–192, 2019.

[48] H. Chart, "*Klebsiella, enterobacter, proteus and other enterobacteria: Pneumonia; urinary tract infection; opportunist infection.* Elsevier Inc., Jul. 2012, pp. 290–297.

[49] W. H. organization (WHO), "Global priority list of antibiotic-resistant bacteria to guide research, discovery, and development of new antibiotics," 2017.

[50] A. Giedraitiene˙, A. Vitkauskiene˙, R. Naginiene˙, and A. Pavilonis, "Antibiotic resistance mechanisms of clinically important bacteria," *Medicina*, vol. 47, no. 3, 2011. [Online]. Available: https://www.mdpi.com/1648-9144/47/3/19

[51] J. W. Costerton, P. S. Stewart, and E. P. Greenberg, "Bacterial biofilms: A common cause of persistent infections," *Science*, vol. 284, no. 5418, pp. 1318–1322, 1999. [Online]. Available: https://www.science.org/doi/abs/10.1126/science.284.5418.1318

[52] V. Puca, R. Z. Marulli, R. Grande, I. Vitale, A. Niro, G. Molinaro, S. Prezioso, R. Muraro, and P. Di Giovanni, "Microbial species isolated from infected wounds and antimicrobial resistance analysis: Data emerging from a three-years retrospective study," *Antibiotics*, vol. 10, no. 10, 2021. [Online]. Available: https://www.mdpi.com/2079-6382/10/10/1162

[53] A. P. Magalhães, N. F. Azevedo, M. O. Pereira, and S. P. Lopes, "The cystic fibrosis microbiome in an ecological perspective and its impact in antibiotic therapy," *Applied microbiology and biotechnology*, vol. 100, pp. 1163–1181, 2016.

[54] A. P. Magalhães, S. P. Lopes, and M. O. Pereira, "Insights into cystic fibrosis polymicrobial consortia: the role of species interactions in biofilm development, phenotype, and response to in-use antibiotics," *Frontiers in Microbiology*, vol. 7, p. 2146, 2017.

[55] S. P. Lopes, N. F. Azevedo, M. O. Pereira et al., "Emergent bacteria in cystic fibrosis: *in vitro* biofilm formation and resilience under variable oxygen conditions," *Biomed Research International*, vol. 2014, 2014.

[56] P. J. Planet, "Adaptation and evolution of pathogens in the cystic fibrosis lung," *Journal of the Pediatric Infectious Diseases Society*, vol. 11, no. Supplement_2, pp. S23–S31, 2022.

[57] G. Khanbabaee, M. Akbarizadeh, A. Sayyari, M. Ashayeri-Panah, F. Abdollahgorji, K. Sheibani, and N. Rezaei, "A survey on pulmonary pathogens and their antibiotic susceptibility among cystic fibrosis patients," *The Brazilian Journal of Infectious Diseases*, vol. 16, no. 2, pp. 122–128, 2012.

[58] R. Rafiee, F. Eftekhar, and S. A. Tabatabaii, "Extended-spectrum β-lactamases in cystic fibrosis isolates of *Klebsiella pneumoniae*," *Jundishapur Journal of Microbiology*, vol. 11, no. 1, 2018.

[59] P. Vali, F. Shahcheraghi, M. Seyfipour, M. A. Zamani, M. R. Allahyar, and M. M. Feizabadi, "Phenotypic and genetic characterization of carbapenemase and esbls producing gram-negative bacteria (gnb) isolated from patients with Cystic Fibrosis (CF) in tehran hospitals," *Journal of clinical and diagnostic research: JCDR*, vol. 8, no. 1, p. 26, 2014.

[60] F. Bittar, H. Richet, J.-C. Dubus, M. Reynaud-Gaubert, N. Stremler, J. Sarles, D. Raoult, and J.-M. Rolain, "Molecular detection of multiple emerging pathogens in sputa from cystic fibrosis patients," *PloS one*, vol. 3, no. 8, p. e2908, 2008.

[61] K. A. McBennett, P. B. Davis, and M. W. Konstan, "Increasing life expectancy in cystic fibrosis: Advances and challenges," *Pediatric pulmonology*, vol. 57, pp. S5–S12, 2022.

[62] A. Françoise and G. Héry-Arnaud, "The microbiome in cystic fibrosis pulmonary disease," Genes, vol. 11, no. 5, p. 536, 2020.

[63] I. A. Janahi and A. Rehman, "The cystic fibrosis airway microbiome and pathogens," *Progress in Understanding Cystic Fibrosis. Rijeka, Croatia: InTech Publishers*, Inc, pp. 45–71, 2017.

[64] C. Li, Y. Wu, A. Riehle, J. Ma, M. Kamler, E. Gulbins, and H. Grassmé, "*Staphylococcus aureus* survives in cystic fibrosis macrophages, forming a reservoir for chronic pneumonia," *Infection and Immunity*, vol. 85, no. 5, pp. 10–1128, 2017.

[65] M. M. Rafeeq and H. A. S. Murad, "Cystic fibrosis: current therapeutic targets and future approaches," *Journal of translational medicine*, vol. 15, no. 1, pp. 1–9, 2017.

[66] N. Høiby, O. Ciofu, and T. Bjarnsholt, "*Pseudomonas aeruginosa* biofilms in cystic fibrosis", *Future microbiology*, vol. 5, no. 11, pp. 1663–1674, 2010.

[67] L. R. Mulcahy, V. M. Isabella, and K. Lewis, "*Pseudomonas aeruginosa* biofilms in disease," *Microbial ecology*, vol. 68, pp. 1–12, 2014.

[68] N. Bagge, O. Ciofu, M. Hentzer, J. I. Campbell, M. Givskov, and N. Høiby, "Constitutive high expression of chromosomal β-lactamase in *Pseudomonas aeruginosa* caused by a new insertion sequence (is 1669) located in ampd," *Antimicrobial agents and chemotherapy*, vol. 46, no. 11, pp. 3406–3411, 2002.

[69] S. P. Lopes, H. Ceri, N. F. Azevedo, and M. O. Pereira, "Antibiotic resistance of mixed biofilms in cystic fibrosis: impact of emerging microorganisms on treatment of infection," *International journal of antimicrobial agents*, vol. 40, no. 3, pp. 260–263, 2012.

[70] A.K.Singh, V.Gaur, and A.K.Maurya, "The role of biofilm in originating, mediating, and proliferating infectious diseases," *Biofilms in Human Diseases: Treatment and Control*, pp. 43–57, 2019.

[71] L.C.Gomes and F.J.Mergulhão,"A selection of platforms to evaluate surface adhesion and biofilm formation in controlled hydrodynamic conditions," *Microorganisms*, vol. 9, no. 9, p. 1993, 2021.

[72] A. S. Azevedo, J. Alljka, S. Kumar, A. Kumar, S. Brás, and C. F. Rodrigues, "*In vitro*, *in vivo*, and *ex vivo* models to study mixed bacterial and fungal biofilms," in *Multispecies Biofilms: Technologically Advanced Methods to Study Microbial Communities*. Springer, 2022, pp. 79–124.

[73] D. d. S. C. M. Castelo-Branco, B. R. Amando, C. J. Ocadaque, L. d. Aguiar, D. D. d. Q. Paiva, E. M. Diógenes, G. M. d. M. Guedes, C. L. Costa, A. S. P. Santos-Filho, A. R. C. d. Andrade et al., "Mini-review: from *in vitro* to *ex vivo* studies: an overview of alternative methods for the study of medical biofilms," *Biofouling*, vol. 36, no. 9, pp. 1129–1148, 2020.

[74] D. S. Auld, P. A. Coassin, N. P. Coussens, P. Hensley, C. Klumpp-Thomas, S. Michael, G. S. Sittampalam, O. J. Trask, B. K. Wagner, J. R. Weidner et al., "Microplate selection and recommended practices in high-throughput screening and quantitative biology," *Assay Guidance Manual* , 2020.

[75] L. C. Gomes and F. J. Mergulhão, "Effects of antibiotic concentration and nutrient medium composition on escherichia coli biofilm formation and green fluorescent protein expression," *FEMS Microbiology Letters*, vol. 364, no. 5, p. fnx042, 2017.

[76] J. Allkja, D. M. Goeres, A. S. Azevedo and N. F. Azevedo, "Interactions of microorganisms within a urinary catheter polymicrobial biofilm model," *Biotechnology and Bioengineering*, vol. 120, no. 1, pp. 239–249, 2023.

[77] H. Almshawit, I. Macreadie, and D. Grando, "A simple and inexpensive device for biofilm analysis," *Journal of microbiological methods*, vol. 98, pp. 59–63, 2014.

[78] E. G. Di Domenico, I. Cavallo, M. Guembe, G. Prignano, M. T. Gallo, V. Bordignon, G. D'Agosto, I. Sperduti, L. Toma, and F. Ensoli, "The clinical biofilm ring test: a promis- ing tool for the clinical assessment of biofilm-producing *Candida* species," *FEMS yeast research*, vol. 18, no. 3, p. foy025, 2018.

[79] E. Mendez, D. K. Walker, J. Vipham, and V. Trinetta, "The use of a cdc biofilm reactor to grow multi-strain listeria monocytogenes biofilm," *Food Microbiology*, vol. 92, p. 103592, 2020.

[80] D. M. Goeres, M. A. Hamilton, N. A. Beck, K. Buckingham-Meyer, J. D. Hilyard, L. R. Loetterle, L. A. Lorenz, D. K. Walker, and P. S. Stewart, "A method for growing a biofilm under low shear at the air–liquid interface using the drip flow biofilm reactor," *Nature protocols*, vol. 4, no. 5, pp. 783–788, 2009.

[81] D. Lebeaux, A. Chauhan, O. Rendueles, and C. Beloin, "From in vitro to *in vivo* models of bacterial biofilm-related infections," *Pathogens*, vol. 2, no. 2, pp. 288–356, 2013.

[82] L. Pedersoli, S. Zhang, F. Briatico-Vangosa, P. Petrini, R. Cardinaels, J. den Toonder, and D. Peneda Pacheco, "Engineered modular microphysiological models of the human airway clearance phenomena," *Biotechnology and Bioengineering*, vol. 118, no. 10, pp. 3898– 3913, 2021.

[83] J. Trevors, "Viable but non-culturable (vbnc) bacteria: gene expression in planktonic and biofilm cells," *Journal of microbiological methods*, vol. 86, no. 2, pp. 266–273, 2011.

[84] S. M. Manohar, P. Shah, and A. Nair, "Flow cytometry: Principles, applications and recent advances," *Bioanalysis*, vol. 13, no. 3, pp. 181–198, 2021.

[85] D. M. Betters, "Use of flow cytometry in clinical practice," *Journal of the advanced practitioner in oncology*, vol. 6, no. 5, p. 435, 2015.

[86] N. Daranas, A. Bonaterra, J. Francés, J. Cabrefiga, E. Montesinos, and E. Badosa, "Monitoring viable cells of the biological control agent lactobacillus plantarum pm411 in aerial plant surfaces by means of a strain-specific viability quantitative pcr method," *Applied and Environmental Microbiology*, vol. 84, no. 10, 2018.

[87] Z.Xu, Y.Liang, S.Lin, D.Chen, B.Li, L.Li, and Y.Deng, "Crystal violet and xtt assays on staphylococcus aureus biofilm quantification," *Current microbiology*, vol. 73, pp. 474–482, 2016.

[88] F. Van den Driessche, P. Rigole, G. Brackman, and T. Coenye, "Optimization of resazurin-based viability staining for quantification of microbial biofilms," *Journal of microbiological methods*, vol. 98, pp. 31–34, 2014.

[89] I. L. E. Barros, F. F. Veiga, J. L. Corrêa, I. C. Jarros, M. Negri, and T. I. E. Svidzinski, "Standardization of resazurin use in susceptibility testing of natural products against yeasts in planktonic cells and in biofilms formation," *Acta Sci. Biol. Sci*, vol. 43, 2021.

[90] C. R. Wensel, J. L. Pluznick, S. L. Salzberg, C. L. Sears et al., "Next-generation sequencing: insights to advance clinical investigations of the microbiome," *The Journal of clinical investigation*, vol. 132, no. 7, 2022.

[91] M. J. Franklin, C. Chang, T. Akiyama, and B. Bothner, "New technologies for studying biofilms," *Microbial Biofilms*, pp. 1–32, 2015.

[92] C. J. Seneviratne, T. Suriyanarayanan, A. S. Widyarman, L. S. Lee, M. Lau, J. Ching, C. Delaney, and G. Ramage, "Multi-omics tools for studying microbial biofilms: current perspectives and future directions," *Critical Reviews in Microbiology*, vol. 46, no. 6, pp. 759–778, 2020.

[93] S. T. Ramírez-Puebla, B. L. Weigel, L. Jack, C. Schlundt, C. A. Pfister, and J. L. Mark Welch, "Spatial organization of the kelp microbiome at micron scales," *Microbiome*, vol. 10, no. 1, pp. 1–20, 2022.

[94] M. Sanderson, I. Smith, I. Parker, and M. Bootman, "Flourescence microscopy," *Cold Spring Harb Protocol*, 2014.

[95] A. Ettinger and T. Wittmann, "Fluorescence live cell imaging," *Methods in cell biology*, vol. 123, pp. 77–94, 2014.

[96] B. Chazotte, "Labeling nuclear DNA using DAPI," *Cold Spring Harb Protoc*, vol. 2011, no. 1, 2011.

[97] H. John, M. Birnstiel, and K. Jones, "RNA-DNA hybrids at the cytological level." *Nature*, vol. 223, no. 5206, 1969.

[98] M. Buongiorno-Nardelli and F. Amaldi, "Autoradiographic detection of molecular hybrids between rrna and dna in tissue sections," *Nature*, vol. 225, no. 5236, pp. 946–948, 1970.

[99] M. L. Pardue and J. G. Gall, "Chromosomal localization of mouse satellite DNA," *Science*, vol. 168, no. 3937, pp. 1356–1358, 1970.

[100] J. Bauman, J. Wiegant, P. Borst, and P. Van Duijn, "A new method for fluorescence microscopical localization of specific DNA sequences by *in situ* hybridization of fluorochrome-labelled RNA," *Experimental cell research*, vol. 128, no. 2, pp. 485–490, 1980.

[101] D. Huber, L. V. Von Voithenberg, and G. V. Kaigala, "Fluorescence *in situ* hybridization (FISH): History, limitations and what to expect from micro-scale FISH?" *Micro and Nano Engineering*, vol. 1, pp. 15–24, 2018.

[102] R. Kandie, R. Ochola, and K. Njaanake, "Evaluation of Fluorescent *in situ* Hybridization technique for diagnosis of malaria in ahero subcounty hospital, Kenya," *BMC Infectious Diseases*, vol. 18, pp. 1–7, 2018.

[103] R. Bishop, "Applications of fluorescence *in situ* hybridization (FISH) in detecting genetic aberrations of medical significance," *Bioscience Horizons*, vol. 3, no. 1, pp. 85–95, 2010.

[104] H. Luo, X. Xu, M. Ye, B. Sheng, and X. Zhu, "The prognostic value of her2 in ovarian cancer: A meta-analysis of observational studies," *PLOS ONE*, vol. 13, no. 1, pp. 1–16, 01 2018. [Online]. Available: https://doi.org/10.1371/journal.pone.0191972

[105] N. Guimaraes, N. Azevedo, C. Figueiredo, C. Keevil, and M. Vieira, "Development and application of a novel peptide nucleic acid probe for the specific detection of helicobacter pylori in gastric biopsy specimens," *Journal of clinical microbiology*, vol. 45, no. 9, pp. 3089–3094, 2007.

[106] N. F. Azevedo and C. Almeida, Fluorescence *in situ* Hybridization (FISH) for *Microbial Cells*, Springer, 2021.

[107] A. S. Azevedo, I. M. Sousa, R. M. Fernandes, N. F. Azevedo, and C. Almeida, "Optimizing Locked Nucleic Acid/2'-O-Methyl-RNA Fluorescence *in situ* Hybridization (LNA/2'OMe-FISH) procedure for bacterial detection," *PLoS One*, vol. 14, no. 5, p. e0217689, 2019.

[108] O. O. Adebowale, S. Goh, and L. Good, "The development of species-specific antisense peptide nucleic acid method for the treatment and detection of viable salmonella," *Heliyon*, vol. 6, no. 6, 2020.

[109] R. Borriss, A. Danchin, C. R. Harwood, C. Médigue, E. P. Rocha, A. Sekowska and D. Vallenet, "Bacillus subtilis, the model gram-positive bacterium: 20 years of annotation refinement," *Microbial biotechnology*, vol. 11, no. 1, pp. 3–17, 2018.

[110] T. J. Silhavy, D. Kahne, and S. Walker, "The bacterial cell envelope", *Cold Spring Harbor perspectives in biology*, vol. 2, no. 5, 2010.

[111] R. Rocha, R. S. Santos, P. Madureira, C. Almeida, and N. F. Azevedo, "Optimization of Peptide Nucleic Acid Fluorescence *in situ* Hybridization (PNA-FISH) for the detection of bacteria: The effect of pH, dextran sulfate and probe concentration," *Journal of biotechnology*, vol. 226, pp. 1–7, 2016.

[112] C. Almeida and N. F. Azevedo, "An introduction to fluorescence *in situ* hybridization in microorganisms," *Fluorescence in situ Hybridization (FISH) for Microbial Cells: Methods and Concepts*, pp. 1–15, 2021.

[113] A. M. Valm, R. Oldenbourg, and G. G. Borisy, "Multiplexed spectral imaging of 120 different fluorescent labels," *PloS one*, vol. 11, no. 7, 2016.

[114] F. Behnam, A. Vilcinskas, M. Wagner, and K. Stoecker, "A straightforward dope (double labeling of oligonucleotide probes)-FISH (Fluorescence *in situ* Hybridization) method for simultaneous multicolor detection of six microbial populations," *Applied and environmental microbiology*, vol. 78, no. 15, pp. 5138–5142, 2012.

[115] A. M. Valm, J. L. M. Welch, and G. G. Borisy, "CLASI-FISH: principles of combinatorial labeling and spectral imaging," *Systematic and applied microbiology*, vol. 35, no. 8, pp. 496–502, 2012.

[116] S. Karkare and D. Bhatnagar, "Promising nucleic acid analogs and mimics: characteristic features and applications of PNA, LNA, and morpholino," *Applied microbiology and biotechnology*, vol. 71, pp. 575–586, 2006.

[117] R. N. Veedu and J. Wengel, "Locked nucleic acid as a novel class of therapeutic agents," *RNA biology*, vol. 6, no. 3, pp. 321–323, 2009.

[118] A. S. Azevedo, C. Almeida, B. Pereira, P. Madureira, J. Wengel, and N. F. Azevedo, "Detection and discrimination of biofilm populations using locked nucleic acid/2-o- methyl-RNA fluorescence *in situ* hybridization (LNA/2'OMe-FISH)," *Biochemical Engineering Journal*, vol. 104, pp. 64–73, 2015, 12th International Chemical and Biological Engineering Conference: Interfacing Bio- and Chemical Engineering. [Online]. Available: https://www.sciencedirect.com/science/article/pii/S1369703X15001667

[119] F. Silvia, B. Joana, M. Pedro, F. Céu, W. Jesper, and A. N. Filipe, "Mismatch discrimination in fluorescent *in situ* hybridization using different types of nucleic acids," *Applied microbiology and biotechnology*, vol. 99, pp. 3961–3969, 2015.

[120] A.S.Azevedo,R.M.Fernandes,A.R.Faria,O.F.Silvestre,J.B.Nieder,C.Lou,J.Wengel, C. Almeida, and N. F. Azevedo, "Spectral imaging and nucleic acid mimics fluorescence *in situ* hybridization (SI-NAM-FISH) for multiplex detection of clinical pathogens," *Frontiers in Microbiology*, vol. 13, p. 976639, 2022.

[121] K. Alam, M. Iqbal, A. Hasan, and N. Al-Maskari, "Rheological characterization of biological hydrogels in aqueous state," *Journal of Applied Biotechnology Reports*, vol. 7, no. 3, pp. 171–175, 2020.

[122] F. Cuomo, M. Cofelice, and F. Lopez, "Rheological characterization of hydrogels from alginate-based nanodispersion," *Polymers*, vol. 11, no. 2, p. 259, 2019.

[123] J. Zhao, P. D. Schloss, L. M. Kalikin, L. A. Carmody, B. K. Foster, J. F. Petrosino, J. D. Cavalcoli, D. R. VanDevanter, S. Murray, J. Z. Li *et al.*, "Decade-long bacterial community dynamics in cystic fibrosis airways," *Proceedings of the National Academy of Sciences*, vol. 109, no. 15, pp. 5809–5814, 2012.

[124] G.B.Rogers,M.P.Carroll,andK.D.Bruce,"Studying bacterial infections through culture-independent approaches," *Journal of medical microbiology*, vol. 58, no. 11, pp. 1401–1418, 2009.

[125] B. Ozel and M. H. Oztop, "Rheology of food hydrogels and organogels," in *Advances in Food Rheology and Its Applications*. Elsevier, 2023, pp. 657–684.

[126] E. M. Ahmed, "Hydrogel: Preparation, characterization, and applications: A review," *Journal of advanced research*, vol. 6, no. 2, pp. 105–121, 2015.

[127] S. Periasamy, H. A. Nair, K. W. Lee, J. Ong, J. Q. Goh, S. Kjelleberg, and S. A. Rice, "*Pseudomonas aeruginosa* PAO1 exopolysaccharides are important for mixed species biofilm community development and stress tolerance," *Frontiers in microbiology*, vol. 6, p. 851, 2015.

[128] S. Singla, K. Harjai, and S. Chhibber, "Susceptibility of different phases of biofilm of *Klebsiella pneumoniae* to three different antibiotics," *The Journal of antibiotics*, vol. 66, no. 2, pp. 61–66, 2013.

[129] K. W. K. Lee, S. Periasamy, M. Mukherjee, C. Xie, S. Kjelleberg, and S. A. Rice, "Biofilm development and enhanced stress resistance of a model, mixed-species community biofilm," *The ISME journal*, vol. 8, no. 4, pp. 894–907, 2014.

[130] R. Hazan, Y.-A. Que, D. Maura, and L. G. Rahme, "A method for high throughput determination of viable bacteria cell counts in 96-well plates," *BMC microbiology*, vol. 12, no. 1, pp. 1–7, 2012.

[131] B. I. Tarnowski, F. G. Spinale, and J. H. Nicholson, "DAPI as a useful stain for nuclear quantitation," *Biotechnic & histochemistry*, vol. 66, no. 6, pp. 296–302, 1991.

[132] B. M. Childers, T. A. VanLaar, T. You, S. Clegg and K. P. Leung, "Mrkd1p from *Klebsiella pneumoniae* strain IA565 allows for coexistence with *Pseudomonas aeruginosa* and protection from protease-mediated biofilm detachment," *Infection and Immunity*, vol. 81, no. 11, pp. 4112–4120, 2013.

[133] E. Reece, P. H. d. A. Bettio, and J. Renwick, "Polymicrobial interactions in the cystic fibrosis airway microbiome impact the antimicrobial susceptibility of *Pseudomonas aeruginosa*," *Antibiotics*, vol. 10, no. 7, p. 827, 2021.

[134] G. Rodríguez-Sevilla, M. García-Coca, D. Romera-García, J. J. Aguilera-Correa, I. Mahíllo-Fernández, J. Esteban, and C. Pérez-Jorge, "Non-tuberculous mycobacteria multispecies biofilms in cystic fibrosis: Development of an in vitro *Mycobacterium abscessus* and *Pseudomonas aeruginosa* dual species biofilm model," *International Journal of Medical Microbiology*, vol. 308, no. 3, pp. 413–423, 2018.

[135] P. S. Stewart, A. K. Camper, S. Handran, C.-T. Huang, and M. Warnecke, "Spatial distribution and coexistence of *Klebsiella pneumoniae* and *Pseudomonas aeruginosa* in biofilms," *Microbial ecology*, vol. 33, pp. 2–10, 1997.

[136] J. Gibson, A. Sood, and D. A. Hogan, "*Pseudomonas aeruginosa-Candida albicans* interactions: localization and fungal toxicity of a phenazine derivative," *Applied and environmental microbiology*, vol. 75, no. 2, pp. 504–513, 2009.

[137] J.-H. Park, J.-H. Lee, M. H. Cho, M. Herzberg, and J. Lee, "Acceleration of protease effect on staphylococcus aureus biofilm dispersal," *FEMS microbiology letters*, vol. 335, no. 1, pp. 31–38, 2012.

[138] F. Alghofaili, "Use of bacterial culture supernatants as anti-biofilm agents against *Pseudomonas aeruginosa* and *Klebsiella pneumoniae*." *European Review for Medical & Pharmacological Sciences*, vol. 26, no. 4, 2022.

[139] K. Zhao, L. Du, J. Lin, Y. Yuan, X. Wang, B. Yue, X. Wang, Y. Guo, Y. Chu, and Y. Zhou, "*Pseudomonas aeruginosa* quorum-sensing and type vi secretion system can direct interspecific coexistence during evolution," *Frontiers in Microbiology*, vol. 9, p. 2287, 2018.

[140] H. Arai, "Regulation and function of versatile aerobic and anaerobic respiratory metabolism in *Pseudomonas aeruginosa*," *Frontiers in microbiology*, vol. 2, p. 103, 2011.

[141] S. S. Yoon, R. F. Hennigan, G. M. Hilliard, U. A. Ochsner, K. Parvatiyar, M. C. Kamani, H. L. Allen, T. R. DeKievit, P. R. Gardner, U. Schwab, J. J. Rowe, B. H. Iglewski, T. R. McDermott, R. P. Mason, D. J. Wozniak, R. E. Hancock, M. R. Parsek, T. L. Noah, R. C. Boucher, and D. J. Hassett, "*Pseudomonas aeruginosa* anaerobic respiration in biofilms: Relationships to cystic fibrosis pathogenesis," *Developmental Cell*, vol. 3, no. 4, pp. 593–603, 2002. [Online]. Available: https://www.sciencedirect.com/science/article/pii/S1534580702002952

[142] P. Chung, "The emerging problems of *Klebsiella pneumoniae* infections: Carbapenem resistance and biofilm formation," *FEMS Microbiology Letters*, vol. 363, p. fnw219, 09 2016.

[143] L.Cerqueira,J.A.Oliveira,A.Nicolau,N.F.Azevedo,andM.J.Vieira,"Biofilm formation with mixed cultures of *Pseudomonas aeruginosa*/*Escherichia coli* on silicone using artificial urine to mimic urinary catheters," *Biofouling*, vol. 29, no. 7, pp. 829–840, 2013.

[144] M. Lakins, J. Marrison, P. O'Toole, and M. Van der Woude, "Exploiting advances in imaging technology to study biofilms by applying multiphoton laser scanning microscopy as an imaging and manipulation tool," *Journal of microscopy*, vol. 235, pp. 128–37, 09 2009.

Appendix A - Aggregates Disruption Tests

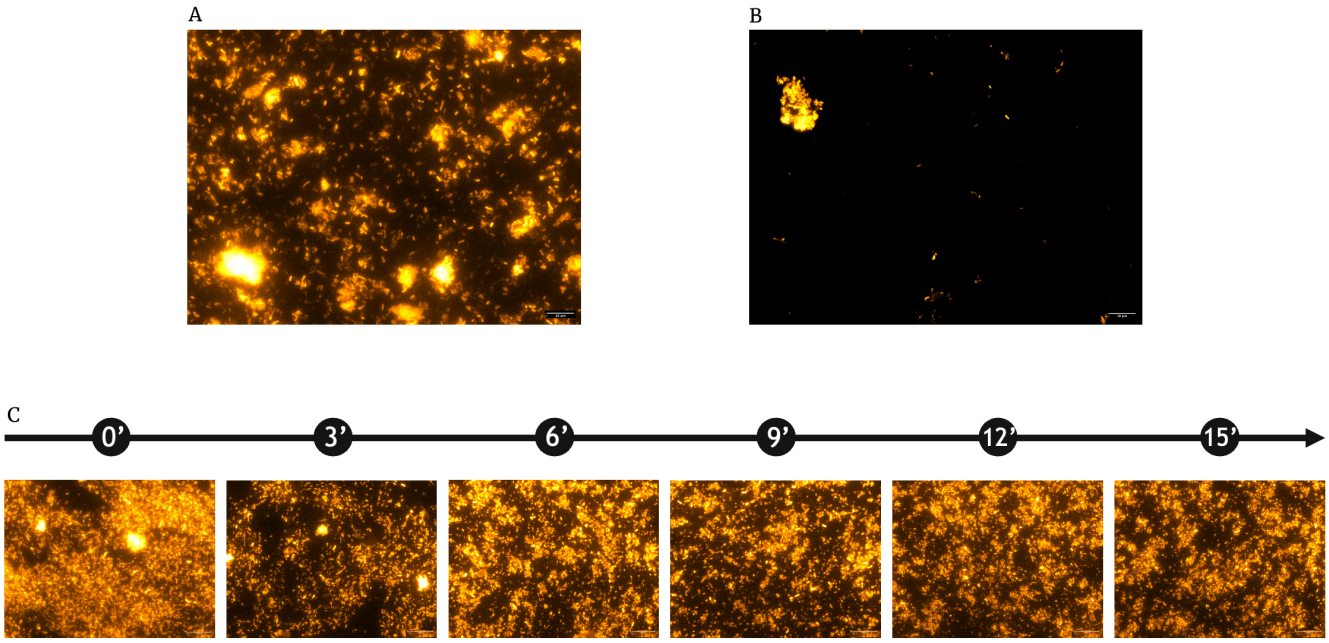

Figure A.1: Aggregates desruption tests. In (A) are the observed cell aggregates, (B) shows the a representative image acquired after treatment with Tween 80 and EDTA and in (C) is the timeline of the acquired images for the different ultrasound bath times, revealing no aggregates at a minimum time of 6 min.